The Pennsylvania State University

The Graduate School

Department of Energy and Mineral Engineering

THE INTERACTION OF SYNTHETIC PETCOKE SLAGS WITH ALUMINA CRUCIBLES

A Thesis in

Energy and Mineral Engineering

by

Kashyap Karri

Submitted in Partial Fulfillment
of the Requirements
for the Degree of

Master of Science

December 2018

The thesis of Kashyap Karri was reviewed and approved* by the following:

Sarma V. Pisupati
Professor of Energy and Mineral Engineering
Thesis Advisor

Mark Klima
Associate Professor of Mineral Processing and Geo-Environmental Engineering

Mohammad Rezaee
Assistant Professor of Mining Engineering

Luis Ayala
Professor of Petroleum and Natural Gas Engineering
Associate Department Head for Graduate Education

*Signatures are on file in the Graduate School

ABSTRACT

Entrained flow gasifiers generate ash as a byproduct while producing syngas. The high temperature inside the gasifier melts the ash and the resulting slag flows down along the refractory-lined (usually high alumina) walls of the gasifier. During high temperature viscosity measurement experiments simulating the conditions found inside gasifiers, it was found that the walls of the crucible, made of alumina lost thickness and developed perforations that cause the molten slag to leak out.

The problem of depletion of refractory material when in contact with molten petcoke ash slags was investigated using thermodynamic equilibrium calculation software FactSage™ to identify the cause. Simulations were performed using synthetic petroleum coke ash slags in high density alumina crucibles. During the simulations to identify the thermodynamically stable phases at various temperatures in 1050-1650°C range, it was found that if the amount of alumina present in the initial slag was less than the equilibrium value, then the alumina from the crucible was dissolved into the slag reaching the equilibrium levels. Dissolution of alumina was however, found to be dependent on the atmosphere in which the slag was heated. Simulations carried out in 100%H_2, 5% H_2/ 95% N_2, 69.5% CO/ 30.5% CO_2 and 100% O_2 atmospheres showed that pure H_2 atmosphere produced the least amount of alumina at equilibrium, suggesting that the atmosphere played a role in dissolution of alumina from the crucible.

The simulations with varying contents of alumina suggested that a deficit of alumina in the starting mix favored the slag picking it up from the crucible. This hypothesis was tested experimentally by heating a synthetic slag mixture containing higher amount of alumina to 1500°C in 5% H_2/N_2 atmosphere, thus simulating the conditions encountered during the viscosity measurement experiment. During FactSage™ simulations, it was observed that 5% H_2/N_2 mixture was as reducing atmosphere as CO/CO_2 (30.5%:69.5%) from the perspective of alumina dissolution into the slag. This was confirmed by x-ray diffraction (XRD) analysis of the two samples, as the patterns revealed the existence of similar compounds (anorthite, corundum, and crystobalite) in the bulk of the slags in both cases.

Scanning electron microscopy- energy dispersive spectrum (SEM-EDS) analysis of the samples showed that the ash sample with lower initial content of alumina showed higher amounts of aluminum at the slag-crucible interface, thus confirming the hypothesis, while the concentration

of alumina in the other case was very low, indicating very little, if any dissolution from the crucible surface.

This study suggests that addition of alumina-rich material to slags with lower alumina contents helps minimize the interaction of slag with the refractory wall and its degradation. This leads to lower depletion of alumina from the wall material and reduces the degradation of refractory walls.

TABLE OF CONTENTS

List of Figures vi

List of Tables viii

Acknowledgments ix

Chapter 1 INTRODUCTION 1

1.1 Gasifier Operations 2
1.2 Slag Viscosity 4
1.2.1 Impact of Composition on Slag Viscosity 5
1.2.2 Impact of Atmosphere on Viscosity 7
1.2.3 Impact of Cooling Rates 8

Chapter 2 LITERATURE REVIEW 9

2.1 Factors Affecting Slag Viscosity 9
2.2 Viscosity Prediction/ Data Fitting 11
2.3 Slag-Refractory Interaction 14

Chapter 3 PROBLEM STATEMENT AND METHODOLOGY 16

3.1 Problem Statement 16
3.1 Methodology 16

Chapter 4 EXPERIMENTAL SETUP 18

4.1 Viscometer Setup 18
4.2 Test Matrix 19
4.3 Initial Slag Preparation 20
4.4 Calibration and Measurement 21
4.4.1 Equipment Calibration 21
4.4.2 Slag Viscosity Measurement 22

Chapter 5 RESULTS AND DISCUSSION 24

Chapter 6 CONCLUSIONS 50

REFERENCES 51

APPENDIX A Modified Urbain Equation 54
APPENDIX B Glossary of Terms 55

LIST OF FIGURES

Figure 1-1 Crude oil production in the US (historical) 1

Figure 1-2 Schematic of a typical Gasifier 3

Figure 1-3 Typical viscosity behavior of slags 5

Figure 4-1 Viscometer Setup 18

Figure 4-2 Schematic of the Viscometer 19

Figure 4-3 Heating and cooling profiles used for viscosity measurement. 23

Figure 5-1 Results from the calibration test for published composition [30] 27

Figure 5-2 HV test Viscosity-Temperature correlation (partial) 27

Figure 5-3 LV test Viscosity-Temperature correlation (partial) 28

Figure 5-4 Alumina crucible post viscometer test (perforations are circled) 29

Figure 5-5 Photograph of the perforation used for SEM-EDS analysis 29

Figure 5-6 SEM micrograph of the perforation (HV test) 30

Figure 5-7 EDS pattern at a location close to the perforation (HV test) 31

Figure 5-8 SEM micrograph of the perforation (LV test) 32

Figure 5-9 EDS pattern at a location close to the perforation (LV test) 33

Figure 5-10 SEM micrograph of the crucible bottom (HV test) 34

Figure 5-11 EDS pattern of crucible bottom (HV test) 35

Figure 5-12 SEM micrograph of crucible bottom (LV test) 36

Figure 5-13 EDS pattern of crucible bottom (LV test) 37

Figure 5-14 FactSage™ simulation of synthetic petcoke slag (LV composition). 38

Figure 5-15 FactSage™ simulation of synthetic petcoke slag (high alumina). 40

Figure 5-16 FactSage™ simulation of synthetic petcoke (no alumina). 41

Figure 5-17 FactSage™ simulation of synthetic petcoke (no alumina/ vanadium). 42

Figure 5-18 SEM micrograph of the crucible wall, close to the interface (V test) 44

Figure 5-19 EDS pattern of the crucible close to interface (V test). 45

Figure 5-20 XRD plots for LV and V tests. 46

Figure 5-21 V Test Composition in 10% H_2 47

Figure 5-22 V Test Composition in 20% H_2 47

Figure 5-23 V Test Composition in 25% H_2 48

Figure 5-24 V Test Composition in 50% H_2 48

Figure 5-25 V Test Composition in 75% H_2 49

LIST OF TABLES

Table 4-1 Test oxide compositions 20

Table 5-1 Viscosity data obtained from LV 25

Table 5-2 Viscosity data obtained from HV 25

Table 5-3 Viscosity data from calibration sample 26

ACKNOWLEDGMENTS

I wish to express my heartfelt gratitude to Dr. Sarma Pisupati for accepting me as a graduate student in his research group and for his assistance, guidance and patience during the period of this study. His guidance significantly helped me understand the processes taking place during slag-crucible interactions, especially the chemistry part. His talks also helped me enhance my critical thinking skills while helping me get a hold on my nerves. I also wish to thank Dr. Mark Klima and Dr. Mohammad Rezaee for providing valuable inputs and critical feedback for my work.

I wish to thank Mr. Ronald Wasco, Mr. Brad Maben and other EMS staff members for their help and advice during the course of the study. I would also like to thank Mr. Shubhadeep Banik for his help with the experimental setup for viscosity measurement, Ms. Xiaojing Wang for helping me set up EDS and XRD analyses and Mr. Hari Jammulamadaka for being the constant moral support, helping with the editing of this report and for the discussions that guided my work.

Finally, I would like to express gratitude to my parents, Sambamurty Sastry and Vishala, and brother Kartik for being a constant support and for their unwavering trust in me and my abilities. I would also like to express my gratitude to my wife Sashi for taking care of our daughter singlehandedly while I was busy with the research. Special appreciation goes to my loving daughter Soumya Shriya for being a good girl and not being fussy about her father's absence from her early life.

Last but definitely not the least, I would like to thank my uncle Ravi Maruvada and aunt Aruna Maruvada, without whose emotional support and encouraging talks this work would not have been possible.

Chapter 1
INTRODUCTION

The demand for petroleum fuels in the United States has been on a steady rise since the early 1900s, dropping only for a few years during economic downturns and wars, as shown in Figure 1-1. The current levels of demand are expected to hold steady at least through 2040, per Annual Energy Outlook published in 2016 by the U.S Energy Information Administration.

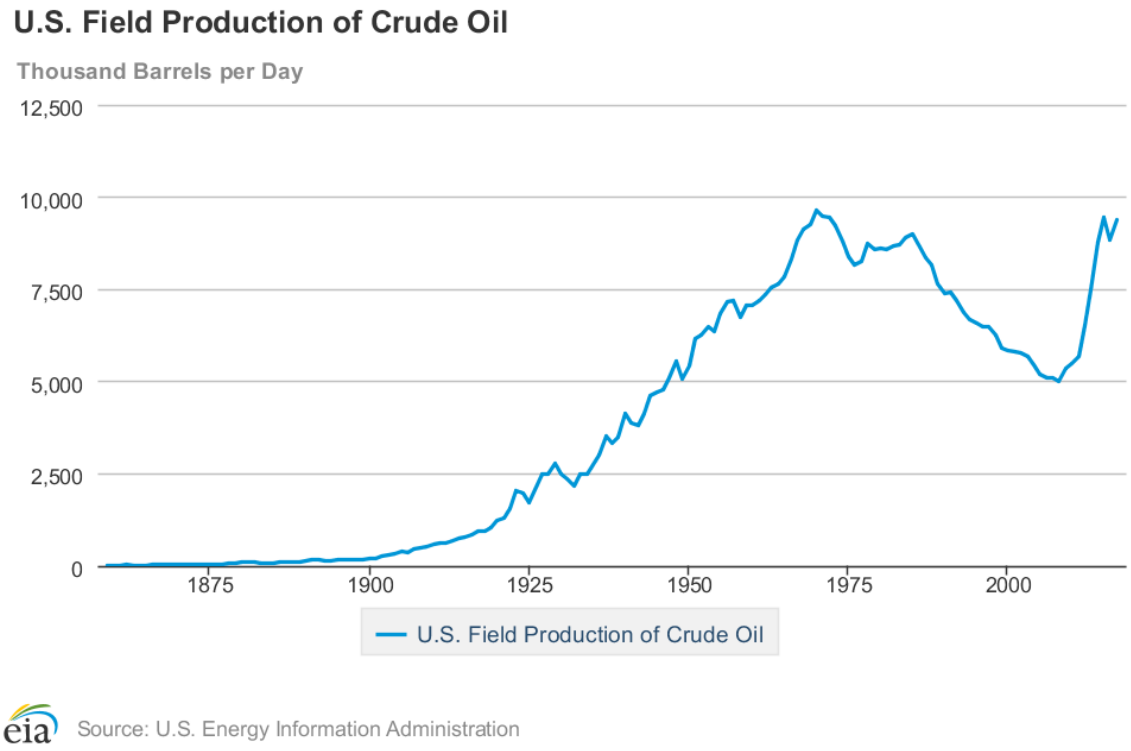

Figure **1-1** Crude oil production in the US (historical)

In response to the increasing demands for petroleum products, there has been a steady rise in the quantity of petroleum being refined. In addition to producing fuels like gasoline, diesels, kerosene, fuel oils, paraffins, liquefied petroleum gas, lubricants, plastics, asphalt and thousands of other products, refining also generates a significant quantity of petroleum coke or petcoke as a byproduct. Petcoke is the carbon-rich residue left over after all the low and medium boiling hydrocarbon fractions have been extracted from the crude oil. This suggests that petcoke, if processed could be a cheap and useful source of energy. This processing is done inside a gasifier,

where solid fuels are converted into a gaseous mixture of CO and H_2, also called synthesis gas or syngas. This syngas is then used as a fuel for electricity generation and synthesis of various petrochemicals and fertilizers. The operation of a typical gasifier is described in the following section.

1.1 Gasifier Operations

There are many technologies employed for achieving the gasification of petcokes. These are: a) fixed/ moving-bed gasifiers, b) fluidized-bed gasifiers, and c) entrained-flow gasifiers [1]. The technology employed is dependent upon the type of petcoke that is to be processed. For example, fixed/moving bed and fluidized-bed gasifier technologies are employed for processing feed containing high quantities of volatile and/ or corrosive components. This is because of the fact that these operate at relatively low temperatures and thus reduce chances of generation of corrosive vapors. Entrained-flow gasifiers operate at higher temperatures and generally achieve better carbon conversion efficiency compared to the other two technologies.

In addition to producing syngas, the gasifiers produce slags that flow towards the bottom where they are removed using a tapping system. A typical gasifier setup is shown in Figure 1-1. All the processes and equipment are shaded in the figure, while all the products are the unshaded cells. The insides of a gasifier are lined with refractory materials that help protect the outsides of the gasifier from the high temperatures generated inside. Owing to the fact that the refractory layer protects the other components from high temperatures, its integrity is of utmost importance in gasifier operations. This becomes even more important in the slagging zone of the gasifier, owing to the fact that the slag has higher contact time with the walls of the gasifier. Highly reactive slags could attack the refractory lining, wearing it faster than lower reactivity slags.

The viscosity of the slags has a marked impact on the rate and ease with which the slag can be tapped out of the gasifier. It is usually assumed that a slag viscosity between 5 Pa.s and 25 Pa.s is ideal for good gasifier slagging operation. Higher viscosities lead to higher residence time of the slag, causing it to be in contact with the refractory for longer and “sticking” to it. This increases the chance of refractory wear significantly. Very high viscosities also could lead to solidification of the slag before tapping and result in clogging of the tapping valve. This could lead to long and expensive repairs, possibly even shutting down of the gasifier unit for extended periods.

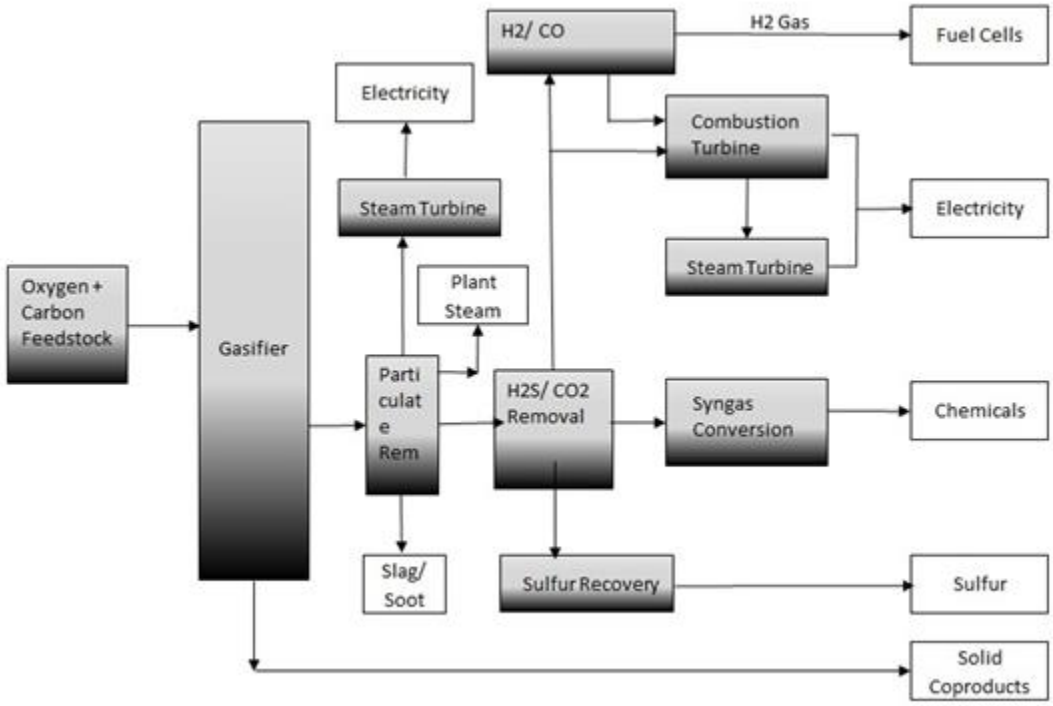

Figure **1-2** Schematic of a typical Gasifier
(Adapted from Bennett et al [2])

Of all the products shown in Figure 1-2, the focus of this study is on the slag generated as residue from gasifier operations. Slag is usually considered a waste product and does not hold any appreciable commercial value. However, the possibility of recovering alkali earth metals like vanadium has piqued the interest of the scientific community in recent times owing to its importance in making various steel and titanium alloys. In small quantities, vanadium makes these metals stronger and more heat resistant. Ferro vanadium alloys are used in the manufacture of gears, crankshafts, and axels whereas titanium-vanadium alloys are used in jet engines, where high temperature resistance is important. Vanadium is found only in small amounts in earth's crust (120 ppm), thus necessitating the recovery/ extraction from commonly used materials like petcoke. Vanadium is found in trace quantities [3] in many types of coals, while its concentration in petcokes can be as high as 79% [4]. These factors make the study of petcoke slag viscosities (for ease of tapping and further processing) important and commercially desirable.

The relationship between slag temperature and viscosity has been researched for a long time and many models, theoretical as well as empirical have been developed for predicting slag viscosities [5]. One reason for the impetus to develop theoretical models is that the experimental determination of viscosity as a function of temperature is not only tedious but also very expensive.

The high temperatures required for the study make it very difficult to precisely determine the viscosities. Some of the critical parameters that determine the temperature-viscosity relationship of a slag are its composition, the type of atmosphere it is subjected to during viscosity measurement, and the rate of cooling of the slag. The effects of these variables are discussed later.

1.2 Slag Viscosity

Viscosity is defined as the property of a fluid to resist shearing forces. If a shearing force is applied to a liquid, it tends to resist the relative motion between the various layers of the fluid. It results from the intermolecular forces and the friction between molecules in the liquid. To flow, the fluid has to be subject to a shear force that is greater than the frictional force between the molecules and/ or the intermolecular forces. At a given velocity of flow, the force required to make the liquid flow is proportional to the fluid's viscosity. Mathematically, the relationship between viscosity, shear stress and shear rate is given as

$$F \alpha A\, v/t,$$

Where F is the shear force acting on a liquid film of thickness t and spread over an area A. v is the velocity of the top surface of the liquid due to F being applied on it. This equation can be written as an equality by introducing a constant μ. Thus,

$$F = \mu\, Av/t$$

Where, μ is called the coefficient of dynamic viscosity and has SI units of Pa.s. v/t is called the shear rate and is expressed in s^{-1}. There are other types of viscosity namely kinematic viscosity and bulk viscosity. However, a discussion on these is beyond the scope of this study.

Depending on their viscosity profiles, fluids can be categorized either as Newtonian or Non-Newtonian. Fluids are said to be Newtonian if, at a given temperature, the shear strain (or shear rate) developed in the fluid is linearly proportional to the shear stress applied. In this case, the stress-strain diagram for the fluid would be a straight line with a zero intercept on the stress axis when the strain is zero. In other words, Newtonian fluids exhibit a constant relationship between applied stress and shear rates observed, which means that subject to a constant stress, the viscosity is a constant.

In non-Newtonian fluids, the shear rate ceases to be proportional to the applied stress. Bingham plastics are materials that exhibit a linear relationship between stress and strain but do not have a zero intercept on the stress axis when the strain is zero. In other words, they act as rigid bodies until a yield stress is applied upon them. Beyond yield stress, the material behaves as a

Newtonian fluid. Shear thinning and shear thickening fluids, as the names suggest display lower and higher viscosities as the applied shear stress is increased and are thus classified as non-Newtonian fluids.

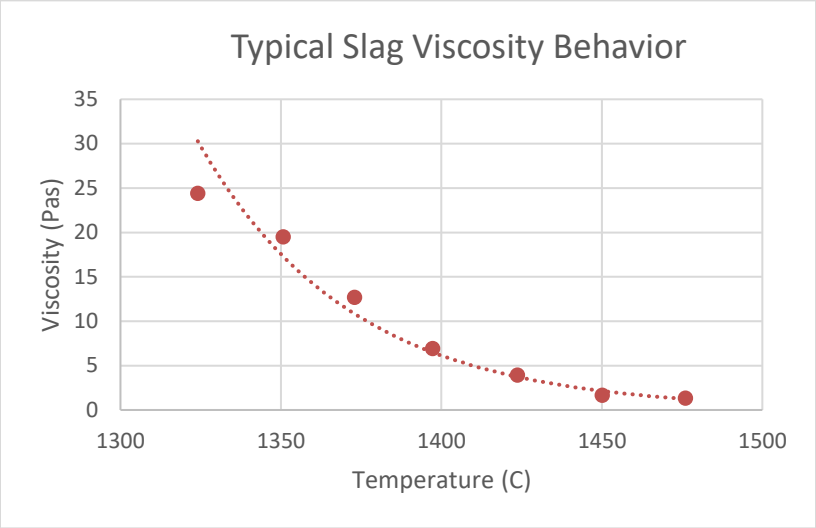

Figure **1-3** Typical viscosity behavior of slags

Coal and petcoke slags above their ash fusion temperatures (AFTs) behave as fluids. Similar to most fluids, they exhibit Newtonian viscosity behavior at higher temperatures, while behaving as non-Newtonian fluids as the temperature decreases. The temperature at which the viscosity of a slag transitions from Newtonian to non-Newtonian is called the temperature of critical viscosity (T_{CV}). The viscosity profile of a slag can broadly be said to be dependent on two factors: its composition and the type of conditions it is subject to (e.g. temperature, atmosphere and the rate of cooling). These effects are discussed in the following sections, with a focus on liquid slags.

1.2.1 Impact of Composition on Slag Viscosity

Slag composition is a critical parameter that determines the slag's response to changes in temperature. Slags containing high melting compounds (V_2O_3, melting point 1940˚C) in sizeable concentrations tend to exhibit non-Newtonian viscosity behavior owing to the existence of multiple phases (liquid-liquid or liquid-solid or more than two phases) more readily than those that have low melting components.

Silica is known to be a glass forming material. When cooled from its molten state (either alone or as part of a slag system), it tends to form long chains of silica tetrahedrons that causes an increase of viscosity. According to the network theory described by Vargas et al. [5], the

constituents of a slag may be classified into one of the three types: network formers, network modifiers, and amphoterics. Network formers, such as Si^{4+}, Ge^{4+} tend to attach themselves within the tetrahedral structure of silicate melts and act as enablers in the formation of longer chains, leading to higher viscosities. Network modifiers like Na^{+}, K^{+}, Mg^{2+}, Ca^{2+}, Fe^{2+}, Cr^{3+}, V^{5+}, Ba^{2+}, Sr^{2+} and Ti^{4+} act to break up the bonds in the tetrahedral structure and reduce the sizes of the chains, resulting in lowering of viscosities. Amphoterics like Al^{3+}, Fe^{3+}, $B^{3+,}$ and Zn^{2+} can act either as network formers or modifiers, depending on their composition in the melt. When the number of modifier ions is comparable to the number of amphoteric ions, they form anions that take positions within the silicates' tetrahedrons, thus acting as network formers. However, if the quantity of modifier ions is not sufficient for charge balance, the amphoterics act as modifiers and reduce slag's viscosity.

There are many models of slags that have been studied over the years. Some of these models are simple binary systems consisting of SiO_2 and another component (Al_2O_3, FeO_x, CaO, MgO, Na_2O, K2O, Li_2O, MnO, TiO_2, B_2O_3 and XCl_x). Others models are ternary, quaternary and quinary systems that include two, three and four components respectively, in addition to SiO_2. The experimental data available for each of these systems have been summarized by Vargas et al. [5].

In binary silicate melts, the size of the second cation (and not SiO_2) determines the viscosity of the mix at lower temperatures and the mobility of the cation at higher temperatures determines the mixture's viscosity. The interactions in higher order systems (ternary, quaternary, etc.) are, however, more complex and have been studied for a long time. As a result, many models that try to predict the viscosity of specific compositions have been used. Some of the most prominent ones are Urbain, Kalmanovitch-Frank (KF), S^2, Riboud, Bottinga-Weill (BW), Watt-Fereday (WF) and Shaw [5].

The biggest drawback of these models, however, is that they are only accurate within certain composition ranges as they were derived on the basis of experiments conducted in those ranges. Beyond the composition that they were designed to be used for, they tend to either overestimate or underestimate viscosities. For example, in the SiO_2 -Fe_2O_3-FeO (0.201-0.004-0.795) system, BW model prediction is the closest to the experimental values obtained by Urbain et al. whereas others predict very different viscosities – on the higher side [5]. However, as the composition changes to 0.371-0.009-0.62 in the results published by Williams et al., the BW model predicts accurate viscosities over a much smaller range of temperatures, with the Shaw model being more accurate for a very small range (1242-1277°C). So, a change in composition led to shrinking of the range of temperatures in which the BW model could predict the viscosity accurately.

Under 1227°C, the viscosity profile is not explained by any of the models studied by the author. Other slag systems also show a similar behavior in that their viscosities cannot be fully predicted using a single model. This explains the existence of so many models of viscosity prediction.

1.2.2 Impact of Atmosphere on Viscosity

It is clear from the discussion on network theory in the previous section that the categorization of Fe as either a modifier or an amphoteric depends on the oxidation state. Under reducing conditions like those found inside gasifiers, Fe almost entirely exists as Fe^{2+} and acts as a modifier while in oxidizing conditions it exists as Fe^{3+}- an amphoteric [5]. Likewise, the atmosphere has a pronounced effect on the oxidation states of vanadium. It exists as V_2O_5 under oxidative conditions, whereas under reducing conditions it exists as V_2O_3 or as V^{3+} in complexes. The melting points of these two oxides are markedly different, with V_2O_5 melting at a far lower temperature than V_2O_3 (690°C vs. 1940°C).

Schobert et al. [6] in their study of coal slags, observed that the viscosities of slags are lower in reducing atmospheres compared to in air (oxidizing atmospheres), partly due to the changes in the oxidation state of Fe. The same logic may be extended to other constituents of the slag that could be present in different oxidation states depending on the atmosphere and influence the slag viscosities differently. Moreover, the presence of water vapor also caused changes in the viscosity of the molten slags.

Zhu et al. [7] highlighted the importance of measurement materials and atmosphere under which measurements are conducted. They discussed the effect of partial pressure of O_2 on the viscosity of coal slags. The viscosity measurements were carried out on synthetic slags resembling the average composition of various Eastern and Western US coals under reducing conditions (partial pressure of O_2 being $10^{-9} – 10^{-7}$ and CO/CO_2 ratio around 1.8).

The effect of atmosphere on the viscosity of slag was studied by Hurley et al. [8]. They determined that coal slag viscosities were lower in reducing atmospheres than in air.

Combustion is an exothermic process whereas gasification is endothermic in nature. As a result, operating temperatures inside a gasifier are higher than those inside a combustor. Moreover, ash melts at lower temperatures under reducing conditions than under oxidizing conditions.

Simulations on FactSage™ for various compositions of slag and under different conditions show very clearly that the composition of the bulk slag (molten slag) at various temperatures is

widely different under different conditions. The presence of oxygen in the atmosphere leads to the formation of different compounds than when the atmosphere is reducing in nature.

1.2.3 Impact of Cooling Rates

Cooling rates affect the crystallization/ solidification and precipitation behavior of the components of the slag. Higher cooling rates appear to cause a more rapid rise in viscosities and higher temperature of critical viscosity (T_{CV}) values than in cases where the slags are subject to more gradual/ slower cooling rates [9]. Higher cooling rates also appear to accelerate the process of refractory degradation and dissolution into the slag. This could cause the slag viscosity to rise rapidly when the slag is in contact for extended time with alumina crucibles/refractory.

Chapter 2
LITERATURE REVIEW

Viscosity measurement is of critical importance in gasification methods/ technologies as the viscosity of the slag generated determines its flow properties and the ease with which it could be removed from the gasifier. There has been substantial research on this subject in the last 45-50 years. However, the more recent focus on the development of clean fuel technologies to minimize the release of CO_2, NO_x, and SO_x has been influential in diverting the attention of scientific community towards coal gasification as a potential pathway to extract more energy from the fuel and reduce emissions.

2.1 Factors Affecting Slag Viscosity

There have been many studies conducted to explain and predict the viscous behavior of slags. Almost all of them deal with metallurgical and coal slags, while petcoke slags' behavior has rarely been studied.

Nakano et al. [10] simplified the analysis of multicomponent systems by maintaining a silica/alumina ratio of 2.23, thereby reducing the number of variables from five to three and vastly reducing the complexity of analysis. The authors studied the effect of CaO and FeO concentration on the solubility of V_2O_3 in slag. The contour plots generated by them suggest that in slags containing higher V_2O_3, the presence of higher concentrations of FeO and CaO helped maintain slag fluidity by enhancing the solubility of V_2O_3 in the bulk of the slag. Their finding also suggests that the presence of higher FeO and CaO prevents crystallization in the slag, thereby expanding the workable/ tapping temperature range for petcoke slags.

However, as the concentration of V_2O_3 in the slag increased beyond 2 wt. %, the authors found more karelianite (V_2O_3) crystals in the slag. These karelianite crystals kept getting bigger with increasing concentration of FeO and CaO. Their work suggests that for every concentration of V_2O_3, there is a unique set of FeO and CaO concentrations where the slag fluidity is at its maximum, even in the presence of appreciable quantities of karelianite crystals. Any change in the concentration of either of these two oxides leads to higher viscosities – all other factors remaining the same.

Zhou et al. [11, 12] proposed that the presence of suspended particles in coal slag has varying effects on its viscosity, depending on the sizes and shapes of the particles. While the viscosity increases with increasing volume fraction of suspended particles, the rise is more rapid and pronounced when the crystals are smaller in size, owing to the ability of smaller particles to pack more efficiently. Moreover, crystal size and shape does not appear to affect the viscosity by much at low volume fractions, whereas the viscosity at higher volume fractions is drastically different – showing dependence on the size and shape of the crystals. Their model is better at viscosity prediction than both Urbain and Watt and Fereday. This model has an advantage over the one proposed by Browning et al. [13] in that the latter model is useful only for prediction of viscosities in the Newtonian region, which means it does not predict viscosities well in slag containing a significant amount of suspended solids.

Duchesne et al. [14] studied the viscosities of various coal and petcoke slags (natural as well as synthetic) and carried out quenching experiments to explain the dynamics involved in the process of slag crystallization and slag-crucible interactions. They also determined that the liquidus temperature of slag is affected by the blending of coal and petcoke ashes. One interesting observation made by the authors is that the liquidus temperature of some coal ashes appeared to be unaffected by addition of V_2O_5, which is in direct contradiction with the findings by Wang et al. [15] who determined that the addition of either vanadium or nickel or both in coal ashes has significant effect on T_{CV}. T_{CV} and liquidus temperature display a strong correlation, as determined by Hsieh et al. [16]. The authors used FactSage™ to calculate the liquidus temperature in their study.

One of the studies that best explains the viscosity-temperature behavior of vanadium-containing slags was carried out by Wang et al. [15] by mixing predetermined amounts of V_2O_5 (4, 7, 10 and 15%) with coal ash. They showed that the presence of vanadium actually lowered the viscosity of the slag at higher temperatures (> 1500°C). The authors explain this apparent anomaly as the result of the reaction between vanadium and alumina to form a solid solution, soaking up free alumina from the bulk slag as a result. Alumina is known as an amphoteric oxide that acts as either a network modifier or as a network former, depending on its concentration and the presence (or absence) or charge stabilizers – oxides that could yield ions to balance the charge on Al^{+3} ions. Excess alumina acts as a network former, increasing the slag viscosity. As the temperature was lowered below 1500°C, slag containing higher vanadium displayed a sharper rise in viscosity owing to precipitation of solid crystals of V_2O_3. Addition of nickel also displayed similar results. Nickel, in its liquid form helped lower the viscosity slightly, while below its melting temperature, it

precipitated as solid and caused a sharp rise in slag viscosity. The presence of a synergistic effect, where vanadium and nickel acted to reduce the T_{CV} of the slag more than when they were added separately was also shown by the authors.

Liu et al. [17] determined that slags that have a high content of CaO and deficit of SiO_2 tend to cause fluctuation in the viscosities due to formation and precipitation of gehlenite. It was also shown that frothing of slags is caused by the presence of SO_3 in the coal ashes, though it has not been supported by any other researchers' findings.

2.2 Viscosity Prediction/ Data Fitting

The modified Urbain equation is widely used for prediction of viscosities of coal slags, owing to its applicability over a wide range of compositions. This equation was developed by Urbain et al. in 1981 from the Weymann equation. This method of viscosity estimation is based on the oxygen contents in the individual components of the slag mixture. The oxides are classified as either glass formers, modifiers or as amphoterics. The equation used for determination of viscosity is

$$\eta = a\, T\, e^{(b.\ 1000)/T}$$

Where a and b are adjustable parameters dependent on the composition of the melt and T is the temperature at which viscosity is being estimated. For detailed discussion on the Modified Urbain equation, please see Appendix B.

It has to be noted that the original equation's coefficients were determined for low viscosity binary and ternary melts and cannot be applied in a similar fashion to high viscosity/ higher order systems. This modification was done by Kalmanovitch and Frank in 1988 [5] for the SiO_2-Al_2O_3-CaO-MgO system by updating the relationship between a and b as

$$-\ln a = 0.2812\, b + 14.1305$$

The above correction to the Urbain equation was found by the authors to be in good agreement with viscosities of various coal samples, but does not help much in predicting the viscosities of petcoke slags as it does not account for the effect of vanadium and nickel in the slags.

The Urbain equation also laid the foundation for the model of viscosity proposed by Srinivasachar et al. [18]. They included the oxidation state of Fe and treated it as a network modifier and predicted the stickiness (or viscosity) of slags with a different composition. The data were then compared with experimental data and the least square error method was used to confirm the validity of their model over the classic Urbain model. They showed that under the conditions of the tests

(reducing atmosphere), it is good to assume that all Fe exists in +2 oxidation state and acts as a network modifier.

Hurst et al. [19, 20] used data obtained from contour plots at various temperatures (1400, 1450 and 1500^0C) to predict the viscosity of coal slags by fitting the empirical viscosity data using the modified Urbain treatment. The values of the coefficients of the modified Urbain equation were shown to be very accurate in predicting the viscosities of the slags at the three temperatures considered.

Kondratiev et al. [21] presented comparison of various metallurgical slag viscosity models, including their effectiveness and limitations of use. The model proposed by them is based on the modified Urbain equation and is useful over a very wide range of compositions. However, it is useful only when working with quaternary systems and has not been tested on higher order ones. Moreover, since it has been proposed for metallurgical slags, it cannot be directly used for petcoke slags.

Kim et al. [22] compared the performance of various viscosity prediction models while studying the flow of slag along the walls of a gasifier. They observed that the Urbain model predicted the lowest viscosity among the five models considered, and that the T_{CV} computed from the Urbain model was the lowest. However, none of the models were able to predict viscosity and T_{CV} satisfactorily.

Oh et al. [23] studied the effect of crystallization on the viscosities of different coal slags and determined that the equation that most closely reflected their viscosity behavior was the one proposed by Annen et al. which is given by

$$\mu_{mixture} = \mu_{liquid} (1+ 2.5c + 9.15 c^2)$$

Where μ_{liquid} was the viscosity of the molten slag determined using the Watt Fereday model for single phase liquids, and c was the solid volume fraction determined theoretically. Another important observation made by the authors was that this fraction assumes that all the solids inside the slag are spherical and thus the equation would only give a rough estimate of the viscosity.

Muller et al. [24] studied the effect of the presence of particles within Newtonian fluids (magma and lava) and determined the relationship between consistency (viscosity in other words) and ϕ, the particle volume fraction as

$$K = (1 - \phi/ \phi_m)^{-2}$$

Where ϕ_m is the maximum particle packing fraction. This equation is similar to the one proposed by Einstein, with a different value for the Einstein coefficient. One advantage of using this equation is that it is applicable to systems containing high solid fractions as well.

The equation for effective viscosity, considering high solid fractions is given as

$$\eta_{eff} = \eta_m (1- \phi/ \phi_m)^{-2.5}, \quad (1)$$

where η_{eff} is the effective viscosity of the liquid-solid mixture, η_m is the actual viscosity of the melt/ viscosity of the suspending medium, ϕ is the volume fraction of crystals in the mix, and ϕ_m is the crystal fraction at which the system transitions into a rigid state

Roscoe also determined the value of ϕ_m for various conditions in which the solid particles could exist inside the mixture. For orderly packed spheres of equal size, ϕ_m assumes a value of about 0.74. For random loose packing, the value is 0.60-0.67. One major hindrance in applying equation (1) is that determination of the exact value of ϕ is not practically feasible. Moreover, the equation also assumes that all the solids are perfect spheres, which again is not a very realistic assumption. Practically, it is not feasible to determine the exact shapes of all the particles and assumptions need to be made for analysis.

Roscoe divided suspensions into three categories namely, very dilute ($\phi = 0.01$ or 0.02), semi-dilute ($0.02 < \phi < 0.25$) and concentrated ($\phi > 0.25$). Of these, the Einstein equation is able to accurately predict viscosities of only very dilute suspensions and progressively deviates as the concentration of solid particles goes higher [25].

Costa [26] proposed a generalized form of the relationship between ϕ and η_{eff} in the Einstein-Roscoe equation by introducing an error function with parameters ϕ , β, γ (all three being adjustable parameters – to be determined empirically) and showed that his function assumes the form of the original Einstein equation for very small ϕ values. One advantage of the equation proposed by Costa is that it is useful for predicting the viscosities even at fairly high values of ϕ, where Einstein-Roscoe equation fails. His work also improves the equation by making it more realistic in the limiting case where the value of ϕ is very close to 1.

Van Dyk et al. [27] used FactSage™ simulations to corroborate experimental determination of viscosities of a blend of six coals ashes and established a method for computation of slag viscosities using the modified Urbain equation. The authors also contend that AFT analysis is not an accurate measure of the slaggability of the ash and that using FactSage™ compositions with the modified Urbain equation would provide viscosities that better match the experimental values. Where the modified Urbain equation uses the average composition to predict slag viscosities, FactSage™ gives the accurate composition at the required temperature.

Wang et al. [28, 29] studied the effect of chemical composition of the ash, additives, atmosphere of operation and their relationship with viscosity. They also showed that AFTs were not a good measure of slag viscosity as coals with similar AFTs could exhibit vastly different

viscosity-temperature profiles, depending on their compositions. They also compared various viscosity prediction models and proposed a model of expressing slag viscosities as a function of temperature, time, composition and shear stress. However, their model was not tested for corroboration with experimental data.

As can be seen from the literature cited above, most of the viscosity prediction models are defined for metallurgical slags, lavas and magmas and coal slags and no accurate prediction model is available for petcoke slags. Adapting the modified Urbain equation to petcoke slags by including the effects of vanadium and nickel on slag viscosity was the motivation for this study

2.3 Slag-Refractory Interaction

High-temperature viscometry is extremely difficult, especially for slags containing high amounts of vanadium due to the aggressive interaction between vanadium and crucible material at elevated temperature. Ilyushechkin et al. [30] determined that slags containing more than 5 wt% vanadium were particularly aggressive in reacting with alumina as well as molybdenum, two of the most suitable materials for the application. Molybdenum crucibles were observed to be affected to a greater extent than alumina crucibles.

French et al. [31] determined that molybdenum reacts weakly with coal slags containing low iron levels (less than 10 wt%), whereas it forms compounds in presence of higher levels of iron, while also generating particles of molybdenum within the molten slag – resulting in slightly higher viscosities being measured. This suggests that molybdenum crucibles and measuring equipment may be used in slags containing low iron. Since this study was on coal slags, the reactivity of vanadium with molybdenum was not explored.

The reactivity of vanadium and molybdenum with crucibles was studied by Ilyushechkin et al. [30], who demonstrated that vanadium reacted aggressively with almost all crucibles, which renders them useless for measurement of viscosities when the slags contain high amounts of vanadium. Of the four crucible materials they studied, molybdenum and alumina were found to be suitable for working with slags containing less than 5 wt. % vanadium, while only alumina crucibles were found to be suited for slags containing more than 21 wt. % vanadium. The authors mentioned that the dissolution of alumina is inevitable and cannot be prevented. As a remedy, the authors suggest designing slags with a deficit in alumina as a way to mitigate the changes in the slag composition. However, it is a general suggestion that does not give any information on how deficit

the slag should be (in alumina) and thus the correct composition would be dependent solely on the operator's experience.

Bennett et al. [2] studied the interaction between slags and chrome lining inside gasifiers. This lining is the surface that is in direct contact with molten slags and is thus most susceptible to damage in the punishing conditions inside the gasifier. They also assert, without any experimental results to back their claim that vanadium (found in petcoke) attacks alumina very aggressively, wearing it out. The authors also claim that FeO from the slag tends to react with Cr_2O_3 lining to form $FeCr_2O_4$ and with Al_2O_3 to form $FeAl_2O_4$. Both these reactions lead to loss of refractory on the slag facing side and thus are major reasons for refractory wear. This is an important factor to consider while choosing the refractory material.

On the basis of the observations by the researchers noted above, alumina crucibles were used for carrying out the measurement of slag viscosities in this study.

Chapter 3
PROBLEM STATEMENT AND METHODOLOGY

3.1 Problem Statement

It was observed during the initial viscosity measurement experiments that some compositions of slag led to very high dissolution of crucible material into the slag, while others did not. It was initially thought that the presence of significant amounts of vanadium had a role to play in the phenomenon, as noted by Bennett et al. [2].

It was also observed that between the two petcoke slag samples with a similar content of vanadium (about 20% by wt.) but with different silica and alumina contents, only one composition caused extensive degradation of the walls of the crucible, while the other did not cause any damage. This led to the inference that vanadium is not the only reason for refractory depletion. To determine if any other factors played a role in this phenomenon, this study focused on the alumina content in the bulk slag as well as the crucible. Since the total alumina in the system (alumina contained in the slag and from the crucible) is constant, any additional alumina predicted or detected in the slag has to come from the crucible, thereby depleting it.

This study investigates the reasons for the dissolution of refractory material, which is mostly alumina into the liquid slag during viscosity measurement experiments, and proposes mitigation measures to minimize the dissolution.

3.1 Methodology

FactSage™, a thermodynamic equilibrium software that predicts the formation of compounds under user defined conditions was used for modeling the conditions and components expected during the viscosity measurement experiments. FactSage™ does this by computing the Gibbs free energy of formation for all possible compounds from the components of the reaction mixture and predicting the formation of those species that result from the reactions that minimize Gibbs free energy.

Four types of slag compositions were tested under 69.5% CO/ 30.5% CO_2, pure H_2, pure O_2 and 5% H_2/N_2 atmospheres. The only variation in the four slag samples was in their alumina and vanadium content, while all other compositions were maintained in the ratio of their presence in

the slag sample that caused extensive dissolution of the crucible. While one composition was similar to the slag sample, another had excess of alumina in its composition. The third composition had no alumina and the fourth had no alumina as well as no vanadium in it.

In the sample with no alumina, presence of alumina, as predicted by FactSage™ must be due to its dissolution from the crucible. Thus a comparison between the first three samples would give us more information about the conditions that lead to dissolution of the alumina from the crucible.

The first step is to determine the extent of alumina that would exist in the slag at equilibrium under the test conditions. This would serve as the basis for classification of slag samples. If the starting sample has less alumina in it than the equilibrium alumina content of the slag, it would indicate that the slag sample was deficient in alumina compared to the equilibrium. Then, an experiment with high alumina slag would show the effect of excess alumina on dissolution.

SEM-EDS, a semi-quantitative method for identification of elemental composition, was carried out to determine the approximate relative presence of the elements in the sample. XRD analysis was used to get the information about the physical structures of the components. A comparison with the FactSage™ simulation data generated by varying the alumina content in the slag would help understand if starting slag's composition has any impact on the phenomenon of dissolution.

Chapter 4
EXPERIMENTAL SETUP

4.1 Viscometer Setup

Viscosity measurements of the synthetic slags were done using a high-temperature viscometer (make: Theta Industries, USA), capable of heating to 1700˚C (Figure 4-1). The setup consisted of the furnace, an alumina protection tube and a glass enclosure for atmosphere control during the experiments, an enclosure for the protection tube, measuring head capable of moving along vertical guide rails, and a rheometer. Three alumina rods fixed to the top of the metal flange were used for holding the crucible in place. Another alumina rod, connected to the rotor at one end with a platinum pin was connected to the measuring head for measuring the shear stress, shear rate, and viscosity. The measuring head consisted of a spring whose deflection indicates the viscosity of the fluid being tested. The metal flange has two sets of perforations, one for letting in the gases into and out of the protection tube and another one for cooling water that prevents the outside of the furnace from overheating.

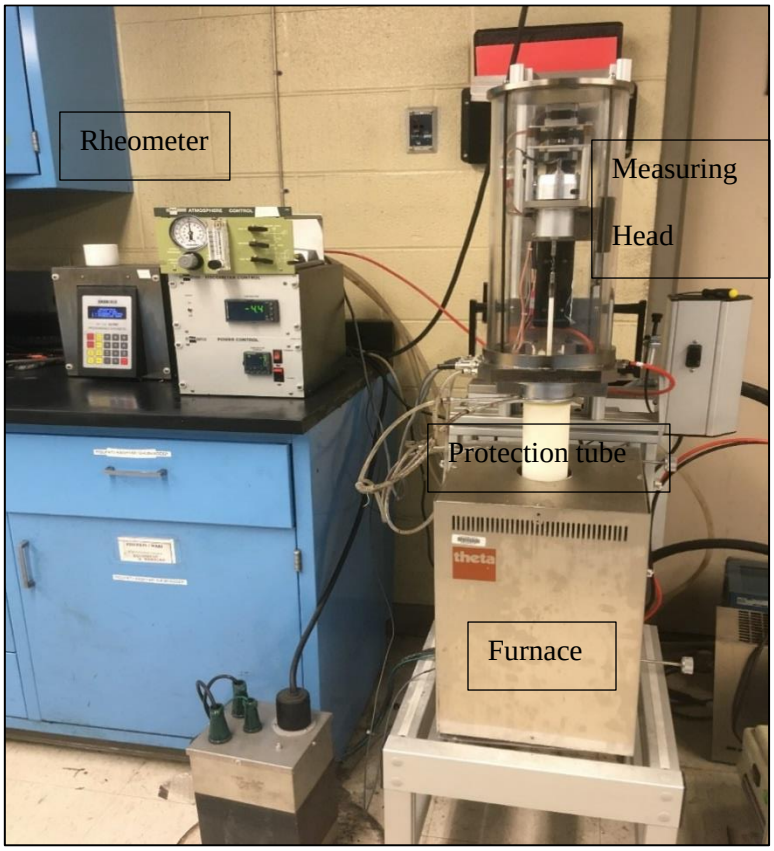

Figure 4-1 Viscometer Setup

A type B thermocouple, in contact with the furnace, was used for reading the furnace temperature, while another type B thermocouple, placed just outside the crucible read the approximate sample temperature. Molybdenum silicide heating elements, embedded into the furnace and capable of providing temperatures up to 1700˚C were used for heating the sample and melting the oxide mixture. Figure 4-2 shows the cross-section schematic of the viscometer in detail.

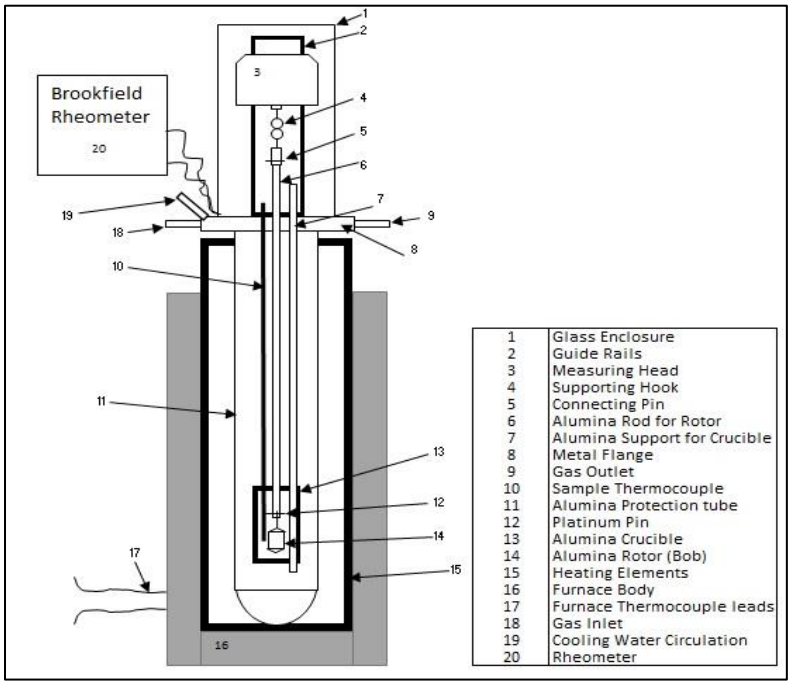

Figure 4-2 Schematic of the Viscometer

4.2 Test Matrix

Six oxides were used in this study: Al_2O_3 (>99% purity, Sigma Aldrich), SiO_2, Fe_2O_3, CaO, NiO and V_2O_5. The process of testing viscosity consisted of two steps –

1) Melting the oxides in an oxidative atmosphere, and

2) Viscosity measurement in reducing atmosphere, mimicking the conditions found inside commercial gasifiers.

The oxides were mixed as per the compositions determined based on the published literature, to match the reported compositions of these respective oxides. The compositions from the nine reported compositions of petcokes by Conn et al [32], Bryers et al [4], Vassilev et al. [33] and summarized by Bennett et al. [2] formed the basis for the composition used during this study. Table 4-1 lists the compositions used for this study.

Table 4-1 Test oxide compositions

Test Type	SiO_2 (g)	Al_2O_3 (g)	Fe_2O_3 (g)	CaO (g)	NiO (g)	V_2O_5(g)	Total
Calibration (C)	43.41	14.82	9.41	4.13	2.68	20.69	95.14*
High V (HV)	14.10	4.80	7.20	5.40	3.00	62.40	96.90
Low V (LV)	23.60	9.40	31.60	8.90	2.90	19.70	96.10
Validation (V)	3.68	9.47	4.93	1.39	0.45	3.08	23.00**

*P2 sample from Duchesne has additional compounds that were added to the oxide mixture but have not been shown here.

**Owing to the size and capacity constraints of the crucible, the test was done with all oxides except Al_2O_3 maintained in the ratio of LV composition.

4.3 Initial Slag Preparation

The crucibles used in this step were procured from Advalue Technology. The crucibles measured 40 mm (Diameter) X 95 mm (height). About 100g of oxide mixture was prepared per test, so as to have sufficient quantity for Step 2. Each crucible was filled with approximately 35g of the mixture to prevent the spilling/ overflowing of the molten mix, in case of foaming/ frothing during the process. Additionally, each crucible was placed inside alumina tubes and covered with alumina lids for containment of any potential spills. The oxides were initially melted under an oxidizing atmosphere in a carbolite box-type furnace, capable of heating to 1700°C to completely oxidize the impurities if any, while also ensuring that all the elements, especially vanadium were in their highest oxidation states for the viscosity measurement tests. The heating and cooling rates were set at 2°C/min and 1.5°C/min respectively, to prevent thermal shock and resultant cracking of the crucibles. The samples were held at 1500°C for 1 minute before being allowed to cool in a controlled manner.

Heating the oxide mixture in oxidizing atmosphere is of particular significance owing to the fact that the melting points of V_2O_5 (~ 690°C) and V_2O_3 (~ 1920°C) are markedly different and exist in different states in the conditions expected during viscosity measurement. Complete conversion of V^{3+} to V^{5+} is extremely important, as the concentration of vanadium used during the experiment would cause significant solids to be present at all temperatures, leading to huge errors in viscosities. It was also instrumental in minimizing foaming and resulting reduction in the volume of the molten slag. This was also necessitated owing to the limitation on the size of alumina crucibles for placing inside the viscometer. Heating in an oxidizing atmosphere also ensured proper mixing of the oxides in their liquid forms.

During one of the trial runs (calibration test) conducted to validate the procedure against previously published literature by Ilyushechkin et al. [30], it was observed that the oxides, if not pre-melted under oxidizing conditions, lost more than 80% of their volume, leading to the viscometer bob being only partially submerged in the melt pool. In the absence of sufficient quantity of molten slag, the bob does not get fully submerged, leading to inaccurate slag viscosity measurement. Moreover, the oxide mixture was found to be much less dense if used directly for viscosity measurement without melting in oxidizing conditions followed by crushing. To give an indication of the difference in the two methods, the crucible could only be filled with 26g of oxides if not previously heated versus about 40g required for proper measurement of viscosity.

4.4 Calibration and Measurement

Measurements of slag viscosity, shear stress, shear rate, and torque were done using Brookfield DV-III rheometer, which provided viscosity values within +/- 1 % of the full range for the selected spindle. This rheometer operates on the principle of measurement of viscous force acting on a spindle rotating at a set constant speed in the fluid being tested. The deflection observed in a calibrated spring through which the spindle passes is used to determine the viscosity of the fluid.

4.4.1 Equipment Calibration

In a rotary viscometer, the viscosity is affected by the relative sizes of the container and the measuring bob that rotates inside the fluid contained in the container. The equipment was calibrated using Standard Reference Material 717a (High Boron Glass) as per the data provided by National Institute of Standards and Technology (NIST) at 1388°C, 1318°C, 1256°C and 1201°C

for the set of rotor bob and crucible described earlier. The data obtained experimentally were matched with the standard data to obtain the correct value of the spindle multiplication constant (SMC). This value of SMC was then set in the rheometer for use during viscosity measurement and was kept unchanged for all subsequent experiments conducted with the same rotor-crucible combination.

4.4.2 Slag Viscosity Measurement

After the box furnace cooled down to room temperature in Step 1, the solidified mix of oxides was separated from the crucible material by carefully breaking the crucible to avoid inclusion of crucible material in the mixture of oxides. Once separated, the mixture was ground in an iron mortar and pestle to powder. This powder was then used for the viscosity measurement step described later in this section.

High alumina crucibles were sourced from Coorstek, USA, as they were claimed to be impermeable to gases and inert towards most chemicals and had high maximum use temperatures (~ 1750˚C). An empty crucible was placed on the alumina supports and the bob was lowered until it touched the bottom. This level was noted down from the scale attached to the measuring head of the equipment, indicating the absolute bottom of the crucible. This also helped identify the height of the slag melt later, before starting the measurements of viscosity by locating the top of the melt pool. The difference between the two levels indicated the height of the molten slag inside the crucible during the experiment.

The powdered mixture weighing about 40-45g was filled in the crucible. This quantity of sample was used to ensure availability of sufficient molten slag for proper immersion of the rotating bob as per the recommendations of the manufacturer. The manufacturer recommended a clearance of at least 3mm between the bottom of the rotor and the bottom wall of the crucible, as well as between the top of the bob and the top of the slag surface to account for end effects during measurement. End effects are caused by the non-availability of sufficient clearance between the bob and the cylinder. This leads to higher viscosity measurement than actual owing to the presence of traction forces, which become significant at low clearances [34]. The height of the bob used was 16mm, its diameter being 12 mm.

A CO/ CO_2 mix (69.5%:30.5%, Praxair, USA) was used for providing the reducing atmosphere necessary to simulate the conditions encountered inside a real-world gasifier. Once the crucible filled with the sample was set on the alumina supporting rods, the rods were lowered into the alumina protection tube. The protection tube was firmly secured to the viscometer’s measuring

head firmly ensuring a gas leak-proof sealing. The viscometer setup was then evacuated using the vacuum pump and filled up with the gas mixture. This step was repeated three times to ensure near-complete removal of air from within the protection tube. After the third filling, the reducing gas supply was cut off.

Figure 4-3 shows the program used for the heating/ cooling process. The furnace was heated until its temperature reached 1600˚C. The temperature of the sample at this point was close to 1500˚C. All the temperatures mentioned henceforth are sample temperatures unless stated otherwise. The sample was held at this temperature for 1 hour to allow for the stabilization of the melt pool to take place. This was done with the spindle raised to its highest position. After stabilization, the spindle was rotated slowly while keeping it above the melt pool. The rotor was then slowly lowered until the torque reading on the rheometer started showing positive, non-zero values. This level was noted from the scale located on the measuring head as the level of the top of the melt pool. The temperatures shown in the plot are furnace temperatures. The temperature read by the thermocouple located next to the sample (sample temperature) was lower than furnace temperature by 100˚C. Thus, the sample temperature was between 1500˚C and 1300˚C during viscosity measurement.

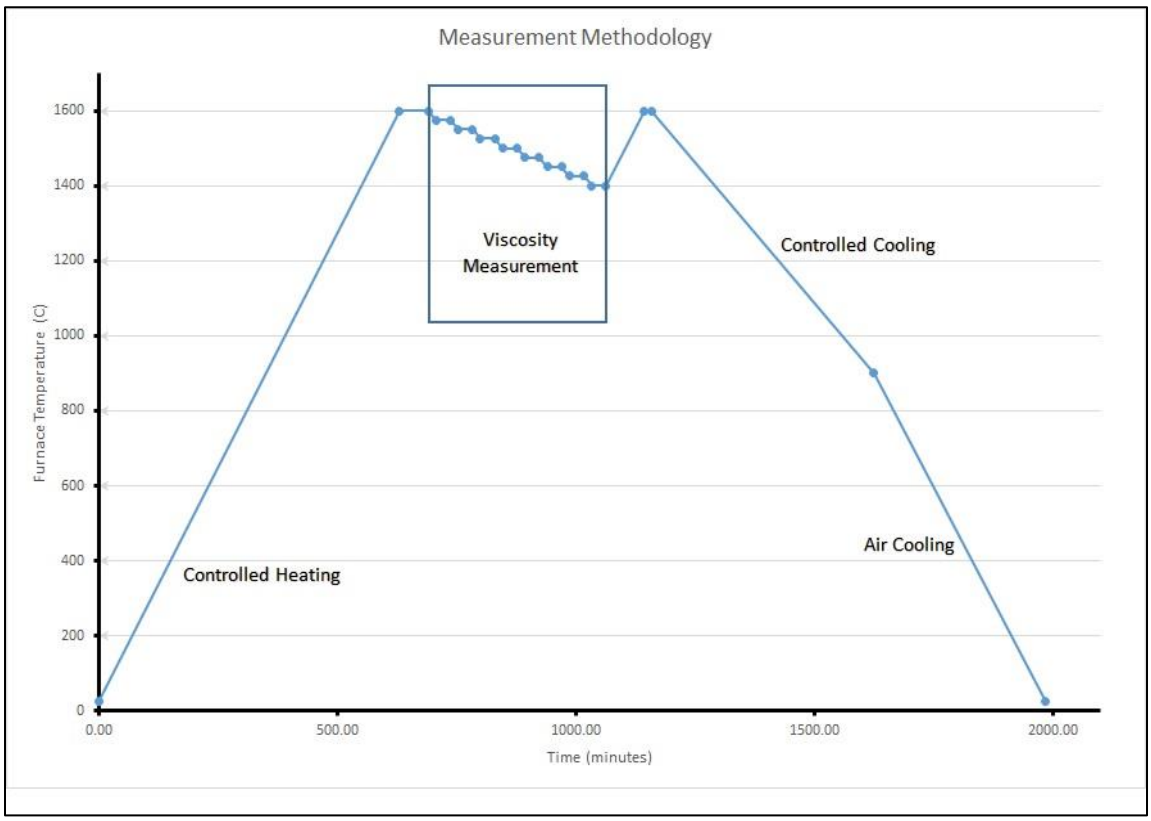

Figure **4-3** Heating and cooling profiles used for viscosity measurement.

Chapter 5
RESULTS AND DISCUSSION

Viscosity measurements in the current study were done for three samples viz. the P2 sample from Duchesne et al. (Calibration Test), HV and LV. The viscosity-temperature plots were generated for the P2 sample detailed by Ilyushechkin et al. [30] (full range) and for the two tests (partly, owing to slag leakage from the crucible). During viscosity measurements for HV and LV samples, parts of the crucibles were found to have dissolved into the slag, leading to complete loss of wall thickness and formation of perforations in the crucibles at two locations. There was no apparent loss of wall thickness during viscosity measurement of the calibration test though its vanadium content was very close to the vanadium content of LV sample. This indicated that the loss of wall thickness was probably not the result of vanadium alone, rather some other interaction between the slag and crucible depleted the alumina. The crucible developed a donut type ring around its circumference, while also getting visibly thinner at that location. Additionally, two perforations were observed in both the cases through which molten slag leaked and fell into the protection tube. Liquid slag falling out of the crucible indicated that the perforations were formed when the slag was fluid enough, most probably at the lower end of the 1,500-1,425˚C temperature range. The lower limit of the 1425˚C was the temperature at which viscosity measurement could no longer be done due to non-availability of slag inside the crucible.

Table 5-1 shows the results obtained from the viscosity measurement experiment conducted on LV sample. As mentioned earlier, readings for lower temperatures were not possible due to non-availability of slag inside the crucible. Table 5-2 shows the results obtained from the viscosity measurement experiment on HV sample, while Table 5-3 shows the results for the calibration sample.

The temperature-viscosity plots generated from tables 5-1, 5-2 and 5-3 are shown in Figures 5-1, 5-2, and 5-3 respectively. Slag viscosity in the calibration run (Figure 5-1) was close to the reported values until 1425˚C, where it started deviating sharply. While it was reported that the sample showed viscosity under 5 Pa.s through about 1275˚C, the viscosity was observed to be higher than 5 Pa.s at all temperatures below 1425˚C. A similar trend was found in the experiment conducted with HV composition (Figure 5-2). However, a comparison of viscosities at similar temperatures for HV and LV samples shows that the viscosities of HV sample (Figure 5-2) were lower than those of LV sample (Figure 5-3) in the range over which measurements could be carried out.

Table 5-1 Viscosity data obtained from LV

Temperature (˚C)	RPM	Stress (D/cm^2)			Strain (s^{-1})
		Minimum	Maximum	Average	
1500.70	5.00	198.00	266.00	232.00	1.25
	10.00	180.00	240.00	210.00	2.50
	15.00	157.00	198.60	177.80	3.75
	18.00	171.20	212.00	191.60	4.50
	20.00	191.20	233.60	212.40	5.00
1474.50	5.00	98.00	268.00	183.00	1.25
	10.00	96.80	184.00	140.40	2.50
	15.00	92.00	174.00	133.00	3.75
	18.00	108.00	169.00	138.50	4.50
	20.00	112.80	174.80	143.80	5.00
1448.50	5.00	129.20	242.40	185.80	1.25
	10.00	96.00	206.00	151.00	2.50
	15.00	96.80	160.30	128.55	3.75
	18.00	98.40	156.40	127.40	4.50
	20.00	97.80	142.60	120.20	5.00

Table 5-2 Viscosity data obtained from HV

Temperature (˚C)	RPM	Stress (D/cm^2)			Strain (s^{-1})
		Minimum	Maximum	Average	
1507.20	30.00	327.50	342.10	334.80	7.50
	25.00	296.30	330.60	313.50	6.30
	20.00	265.70	301.30	283.50	5.00
	15.00	170.30	193.50	181.90	3.80
	10.00	102.30	106.20	104.30	2.50
1478.60	30.00	497.30	538.10	517.70	7.50
	25.00	381.20	417.40	399.30	6.30
	20.00	316.40	343.60	330.00	5.00
	15.00	238.10	297.80	268.00	3.80
	10.00	196.50	212.40	204.50	2.50
1453.40	30.00	681.60	697.10	689.40	7.50
	25.00	612.40	652.30	632.40	6.30
	20.00	498.10	546.20	522.20	5.00
	15.00	298.40	346.70	322.60	3.80

	10.00	238.00	259.70	248.90	2.50
1426.70	25.00	702.10	738.60	720.40	6.30
	20.00	598.30	631.40	614.90	5.00
	15.00	392.10	463.50	427.80	3.80
	10.00	301.30	382.70	342.00	2.50
	7.50	276.10	351.60	313.90	1.90
1401.30	21.00	621.20	668.40	644.80	5.30
	20.00	612.10	645.70	628.90	5.00
	15.00	521.60	583.10	552.40	3.80
	10.00	417.30	463.00	440.20	2.50
	7.50	303.60	384.10	343.90	1.90
1375.60	20.00	793.00	857.00	825.00	5.00
	15.00	609.30	721.40	665.40	3.80
	10.00	532.40	589.60	561.00	2.50
	7.50	412.60	499.30	456.00	1.90
	5.00	321.40	403.10	362.30	1.30

Table 5-3 Viscosity data from calibration sample

Temperature (˚C)	RPM	Stress (D/cm^2)			Strain (s^{-1})
		Minimum	Maximum	Average	
1397.30	20.00	387.20	431.30	409.30	5.00
	15.00	324.60	376.40	350.50	3.80
	10.00	237.40	309.30	273.40	2.50
	7.50	218.40	289.60	254.00	1.90
	5.00	182.40	265.40	223.90	1.30
1372.90	25.00	594.00	632.00	613.00	6.30
	20.00	500.30	537.60	519.00	5.00
	15.00	421.60	468.90	445.30	3.80
	10.00	327.20	408.30	367.80	2.50
	7.50	256.80	341.20	299.00	1.90
1350.70	14.00	716.00	773.00	744.50	3.50
	12.00	632.00	697.00	664.50	3.00
	10.00	550.00	628.00	589.00	2.50
	7.50	459.00	536.00	497.50	1.90
	5.00	348.00	442.00	395.00	1.30
1324.10	10.00	626.00	681.00	653.50	2.50
	8.00	511.00	584.00	547.50	2.00
	7.50	502.40	597.00	549.70	1.90
	5.00	361.60	485.00	423.30	1.30
	4.00	317.00	437.00	377.00	1.00

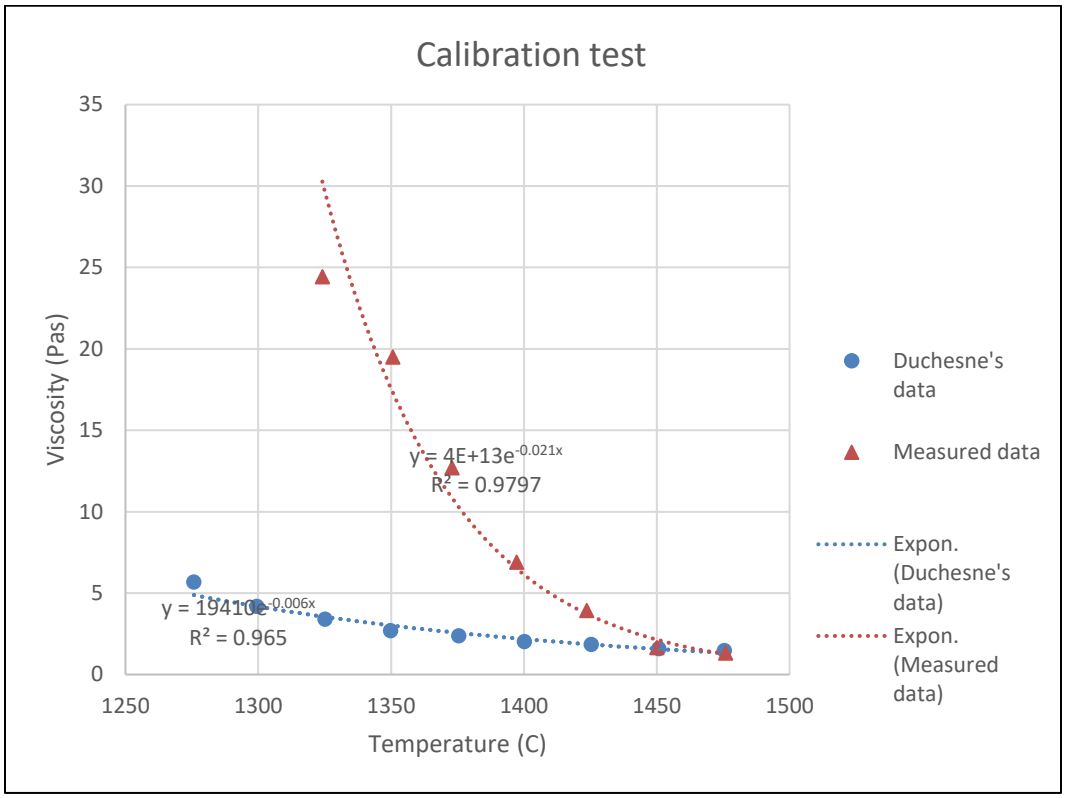

Figure 5-1 Results from the calibration test for published composition [30]

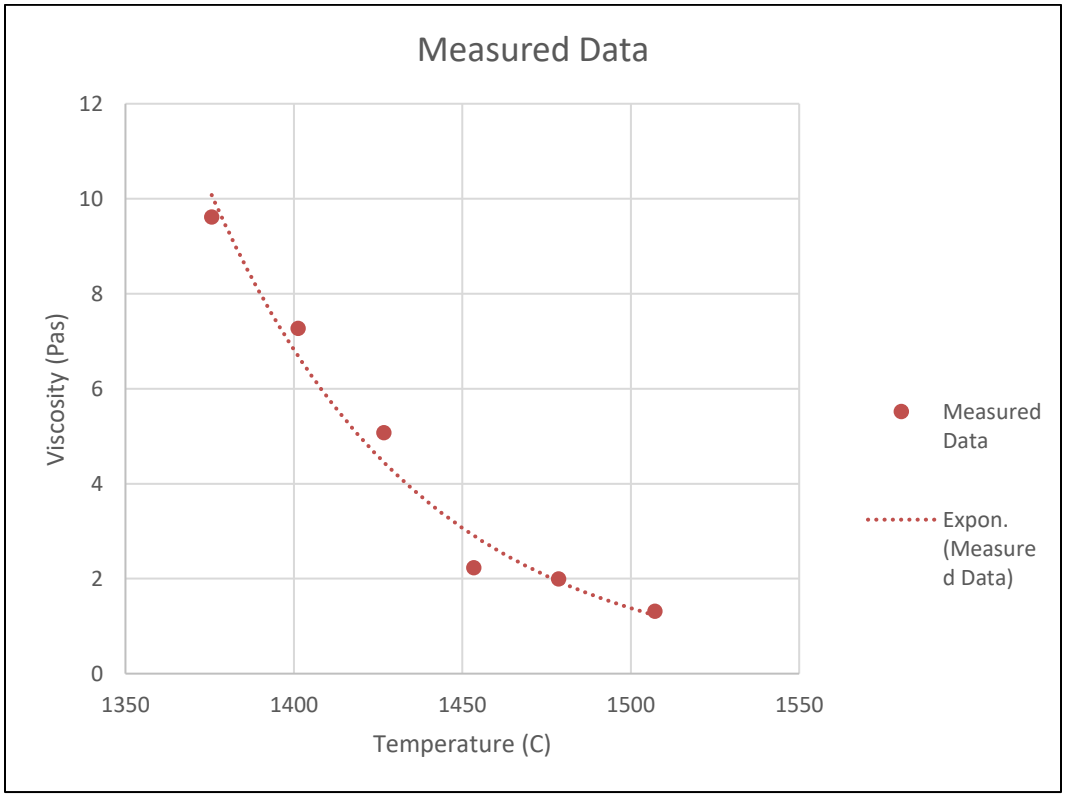

Figure 5-2 HV test Viscosity-Temperature correlation (partial)

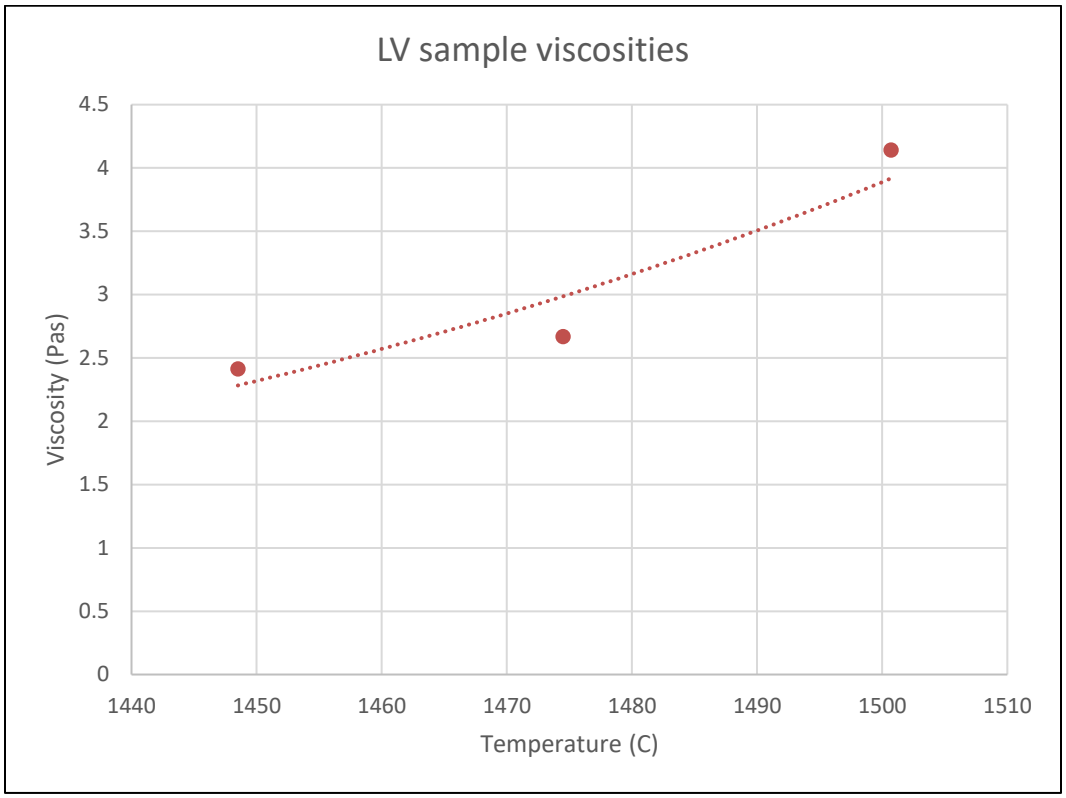

Figure 5-3 LV test Viscosity-Temperature correlation (partial)

Figure 5-3 shows the (partial) data obtained from the viscosity measurement experiment with LV composition. Only three readings were possible before the liquid slag leaked out and no further measurements could be carried out. The viscosity was higher at 1500˚C than in the HV sample (4.2 Pa.s against 1.31 Pa.s) and then reduced to 2.4 Pa.s at about 1450˚C.

Figure 5-4 shows photograph of the crucible after the completion of the viscosity measurement experiment (LV sample). The circumferential swelling and perforations near the bottom of the crucible can be seen here. The bottom of the crucible was swollen all around and was thinner than at the top, indicating depletion of alumina from it. Figure 5-5 shows the photograph of one of the perforations found on the wall of the crucible. Thinning of the wall of the crucible can be noted from this figure.

Figure 5-4 Alumina crucible post viscometer test (perforations are circled)

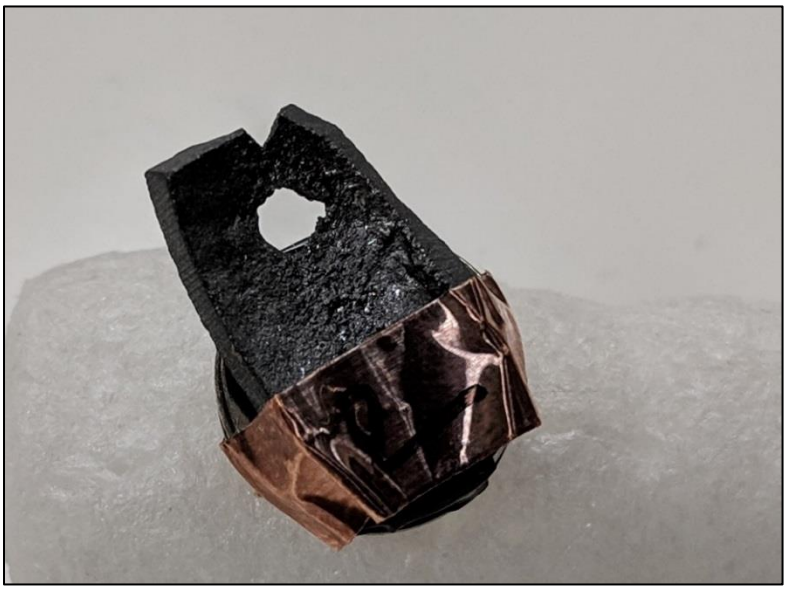

Figure 5-5 Photograph of the perforation used for SEM-EDS analysis

An SEM micrograph of the perforation formed during experiment with HV composition is shown in Figure 5-6. EDS pattern (Figure 5-7) was obtained for a point close to the circumference of the perforation and showed accumulation of vanadium (46.2%), while also showing a lower

content of aluminum (9.9%), down from 32% at the unaffected part of the crucible (Figure 5-10 and 5-11). It must be noted here that SEM is a semi-quantitative technique and the compositions shown here are only for relative composition. They cannot be used as exact compositions.

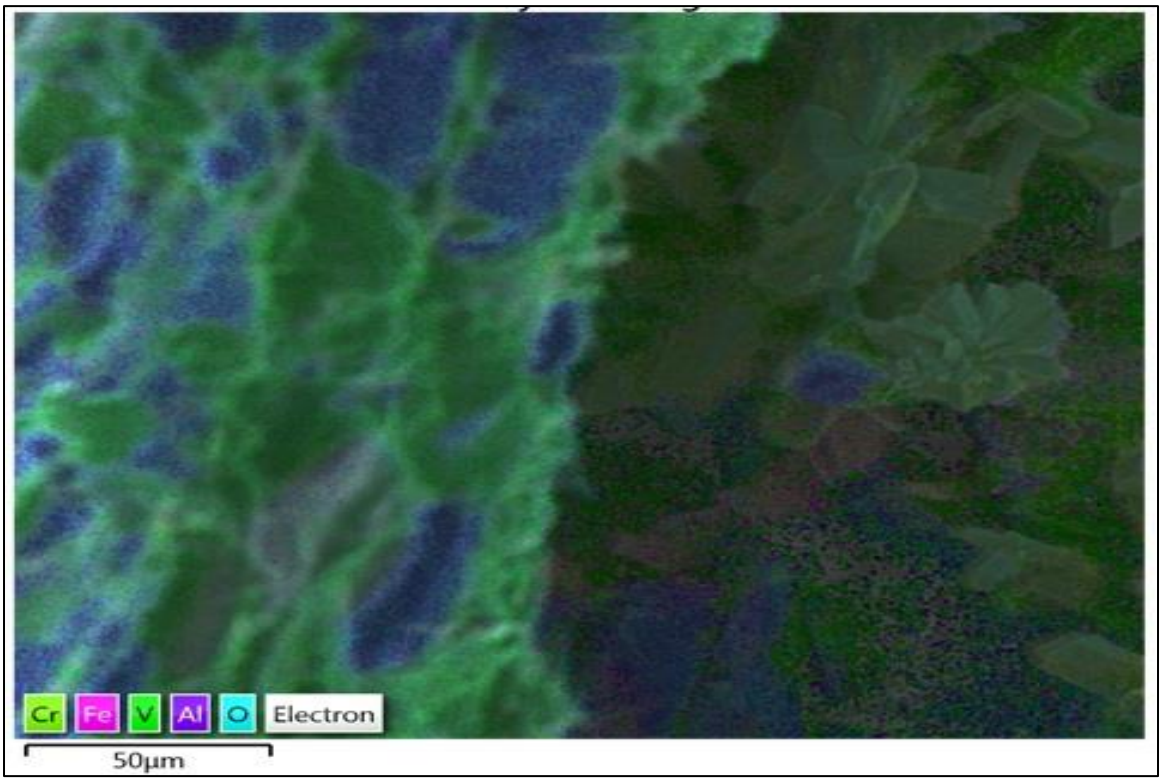

Figure 5-6 SEM micrograph of the perforation (HV test)

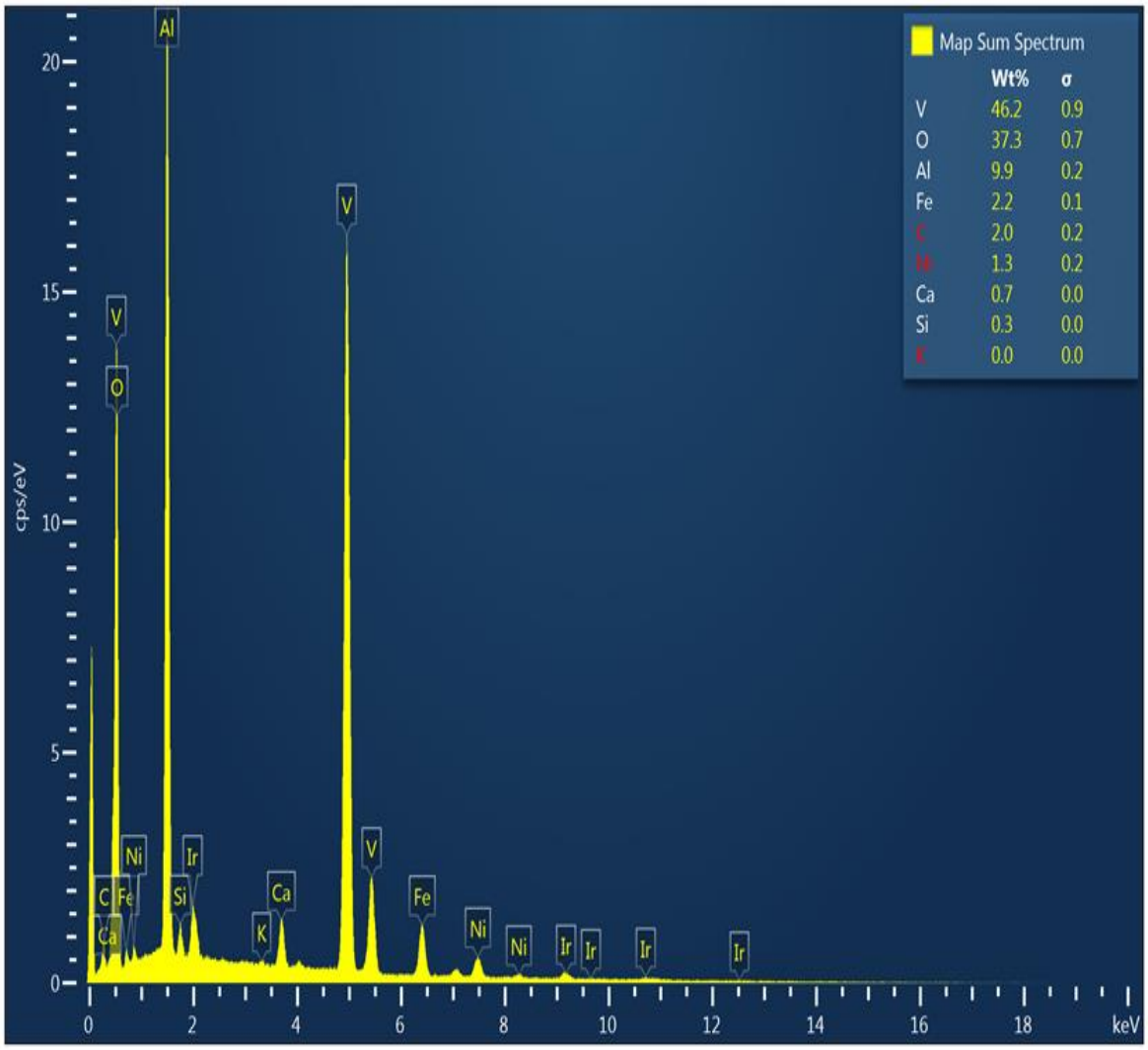

Figure 5-7 EDS pattern at a location close to the perforation (HV test)

Figures 5-8 and 5-9 show the SEM micrograph and EDS pattern at a point close to the perforation found during LV test. These figures also show that there was an accumulation of vanadium close to the perforation accompanied by loss of aluminum. This can be seen from the change in weight percentages of these two elements in the EDS pattern.

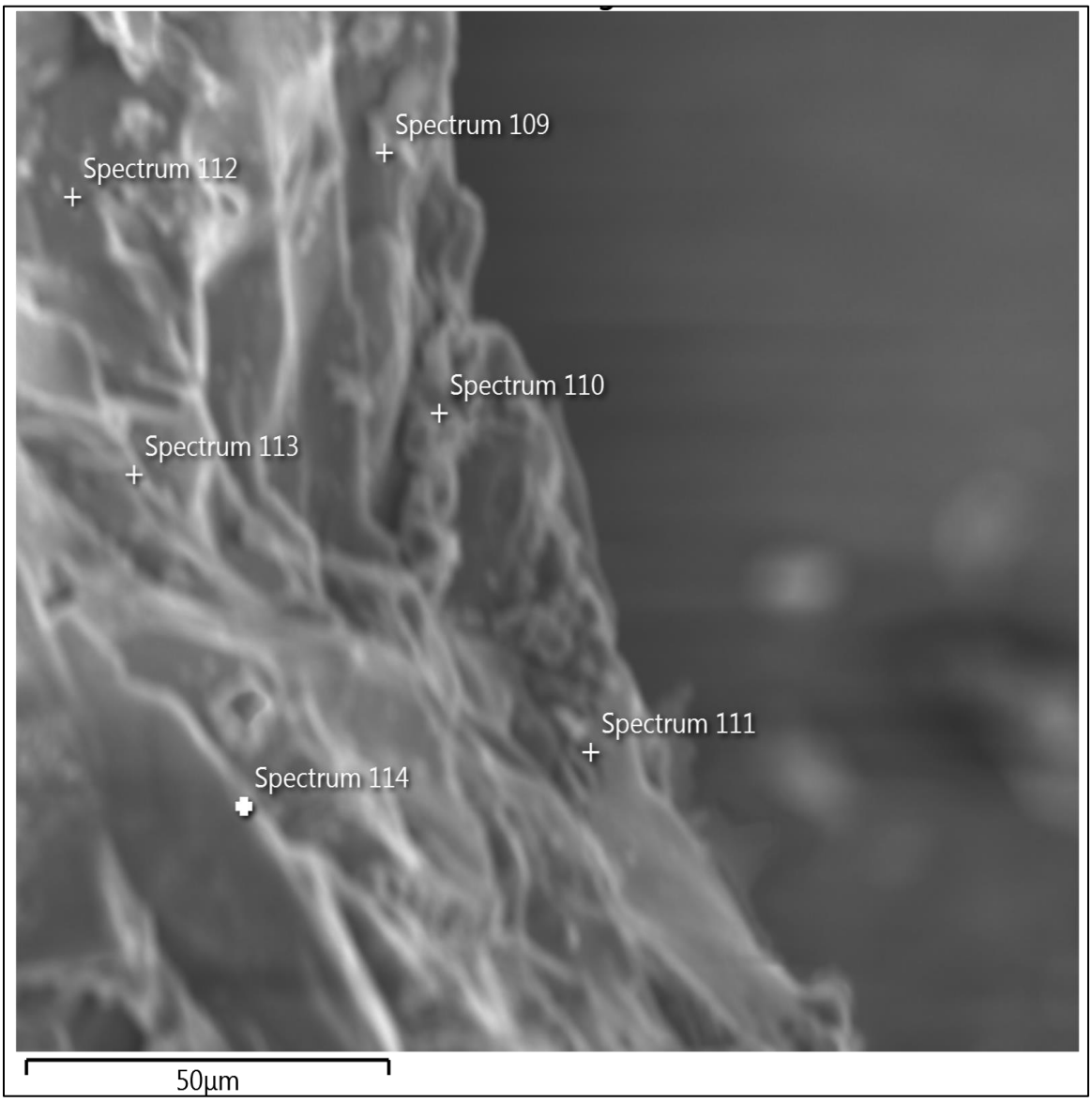

Figure 5-8 SEM micrograph of the perforation (LV test)

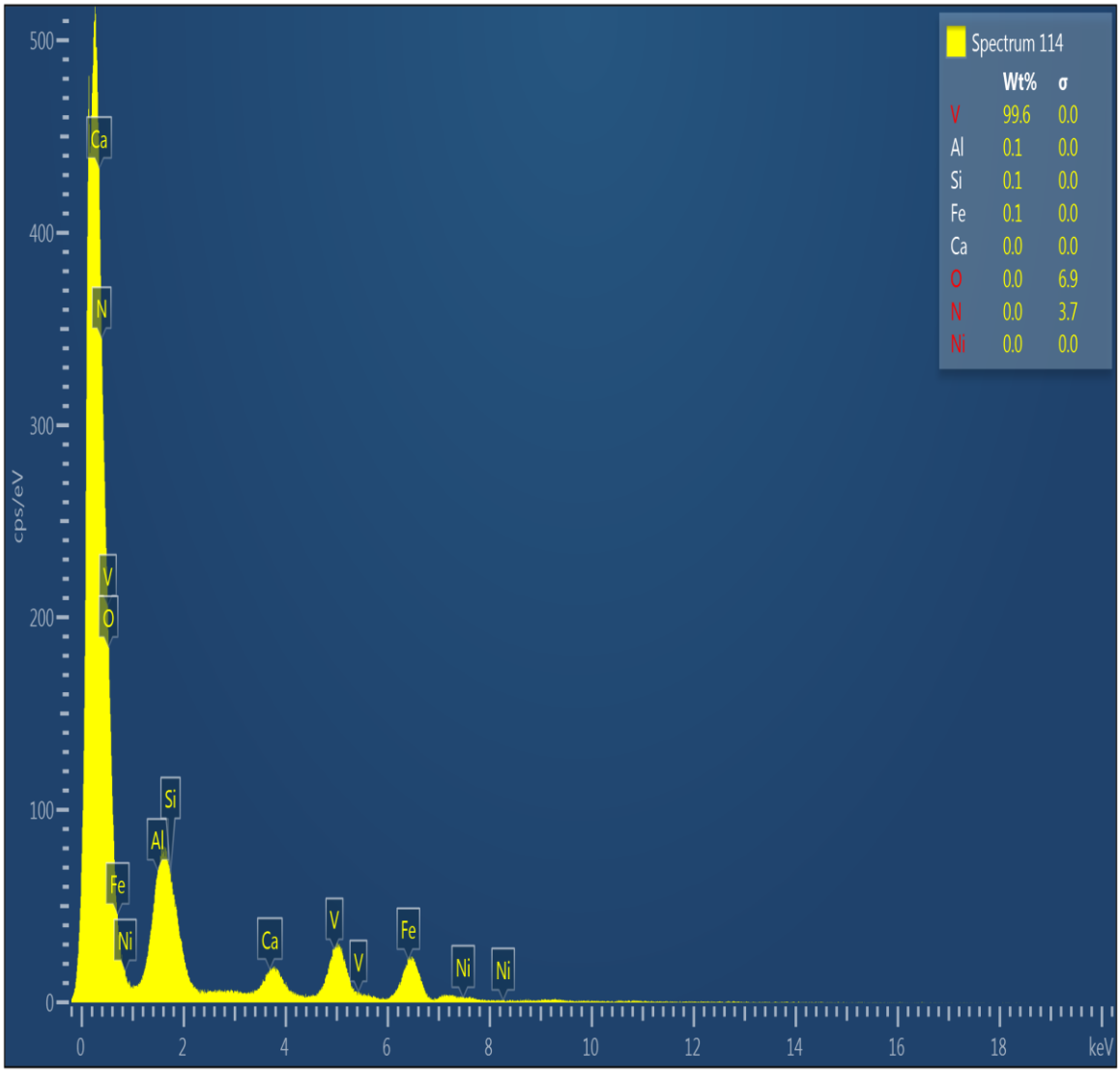

Figure 5-9 EDS pattern at a location close to the perforation (LV test)

Figures 5-10 and 5-11 show the SEM micrograph and EDS pattern from a section of the bottom of the crucible in HV. The bottom of the crucible was not found to have been affected during the experiment. As expected, alumina was the major constituent in the unaffected region of the crucible. Vanadium was identified to be 10.7% by weight at this location, which is a marked difference from the site that developed the perforation (~46%). All other oxide constituents were seen in roughly the same proportions as they were in the starting mixture.

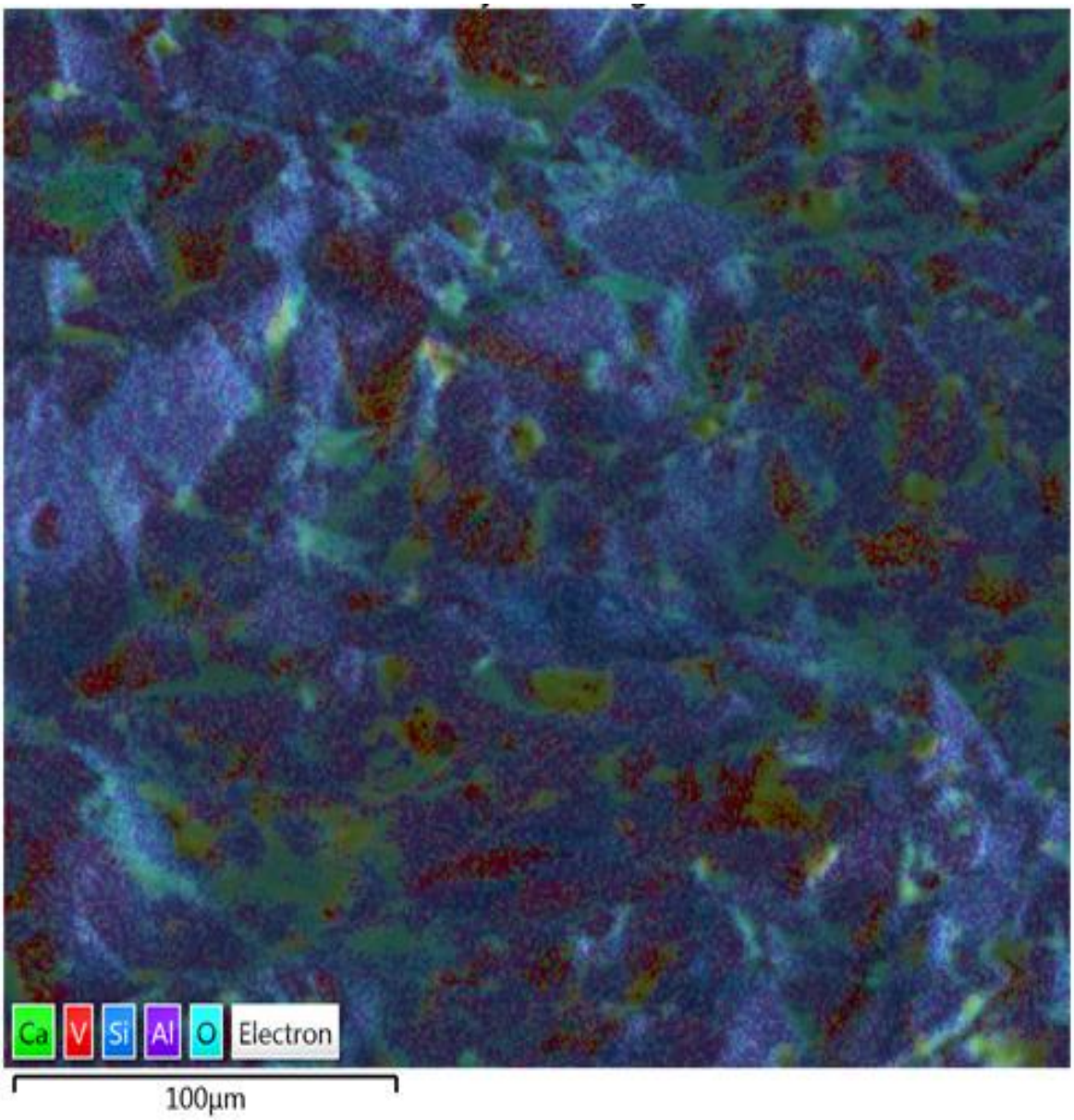

Figure 5-10 SEM micrograph of the crucible bottom (HV test)

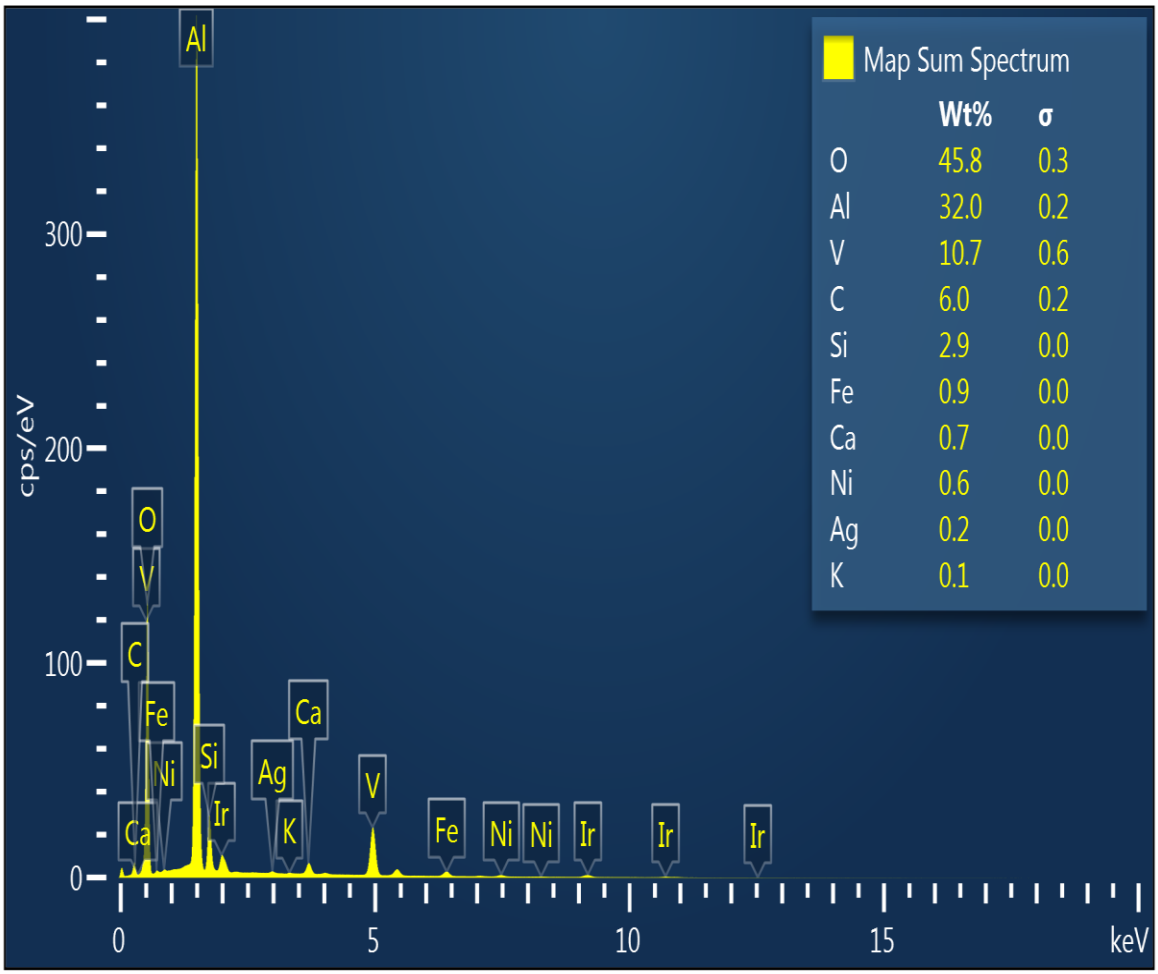

Figure 5-11 EDS pattern of crucible bottom (HV test)

Figure 5-11 also shows the presence of silicon and iron in minute quantities. This could be because of the fact that silica has a low density (2.65 g/cm^3) whereas other oxides are much heavier. Thus, if the slag is maintained in its molten state for long periods, gravity separation of the fluids plays a major role in determining which fluid would be at the top. Since the holes were found at the bottom of the crucibles, it is possible that the heavier oxides escaped first and silica was in contact with the crucible long enough to solidify at the interface before fully flowing out of the hole.

Figures 5-12 and 5-13 show the SEM micrograph and EDS pattern for the bottom of the crucible. The pattern shows a drop in alumina concentration but there was no vanadium detected. Other components like silicon and calcium were also detected.

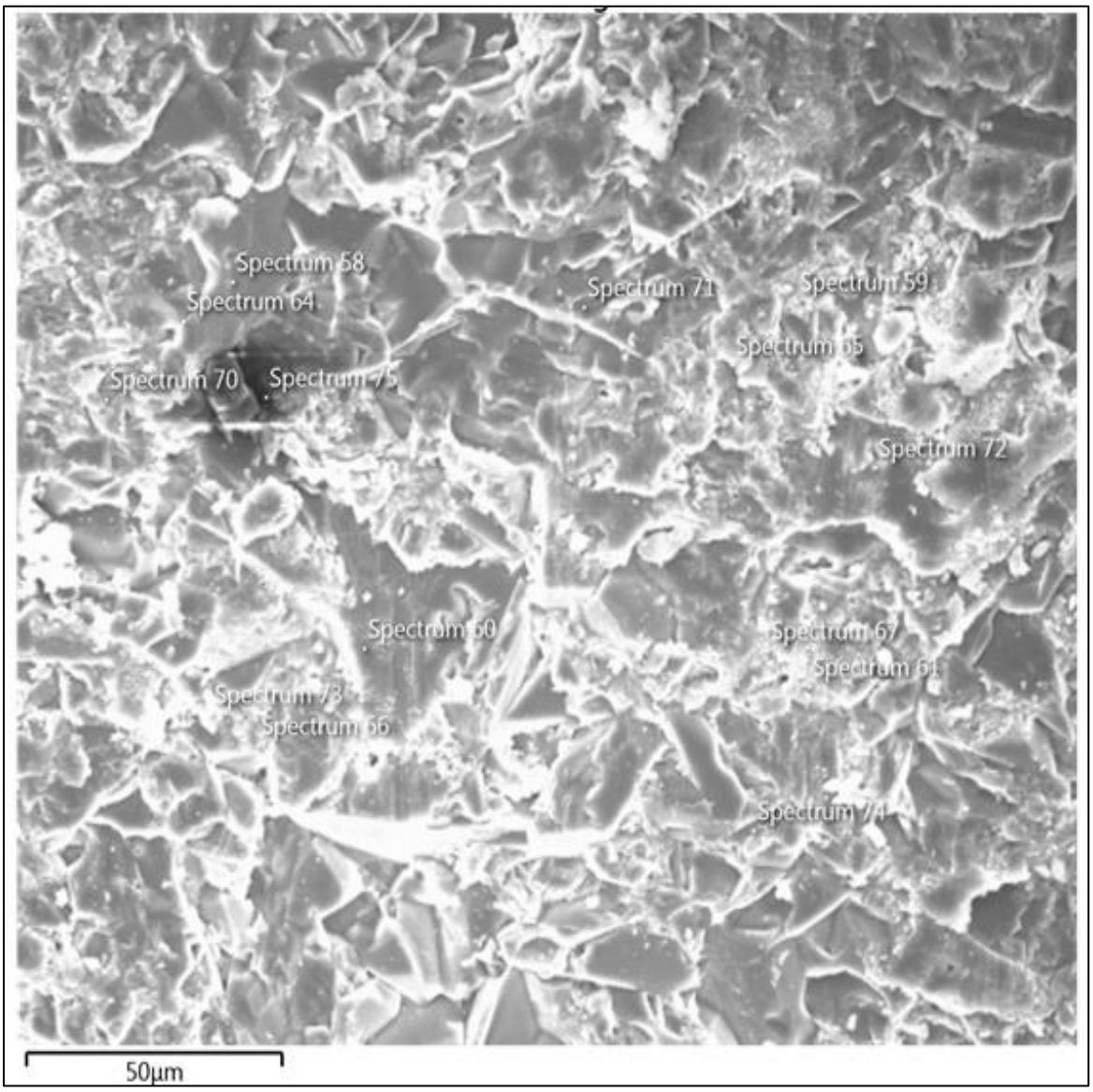

Figure 5-12 SEM micrograph of crucible bottom (LV test)

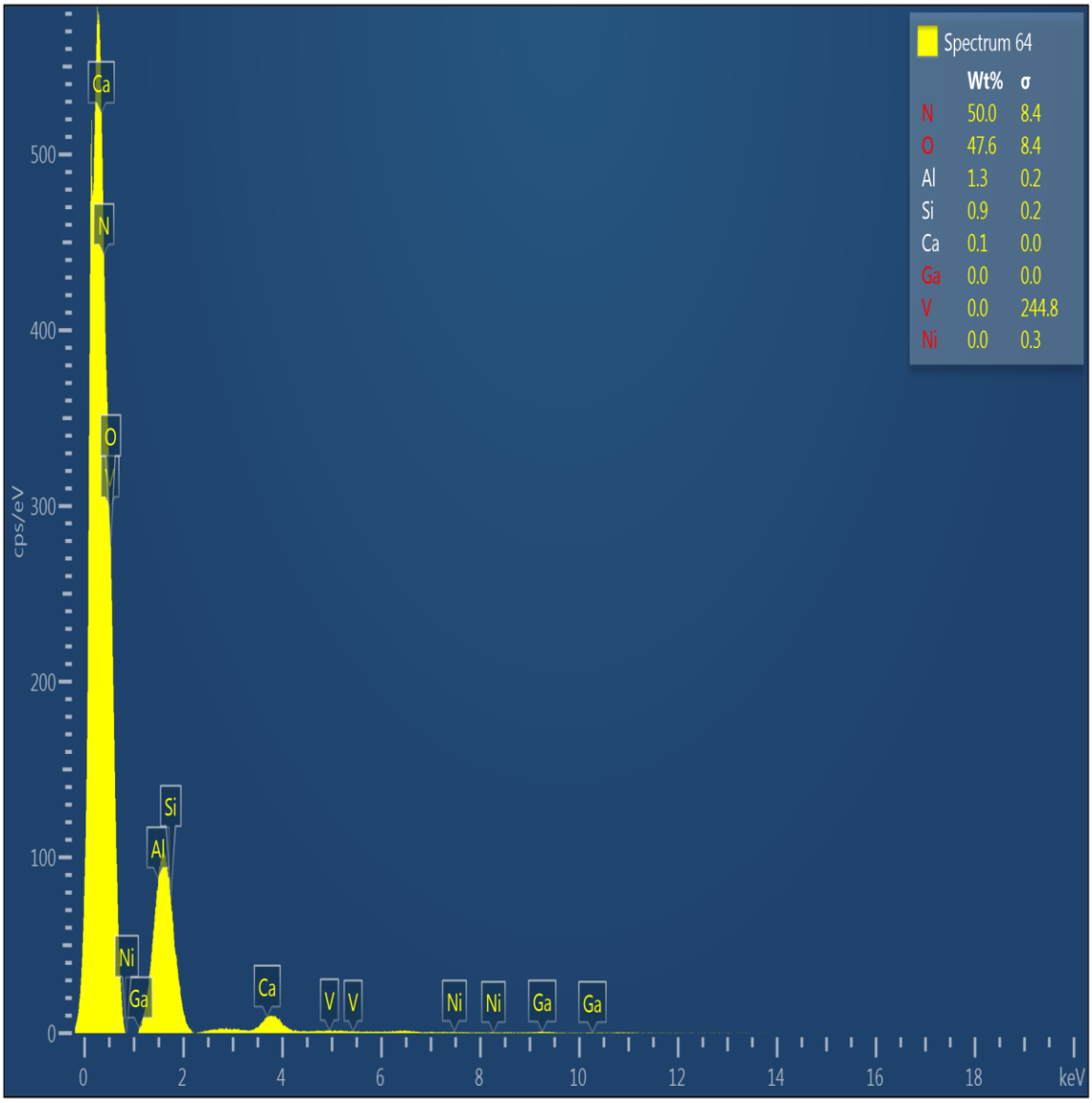

Figure 5-13 EDS pattern of crucible bottom (LV test)

Figures 5-14 through 5-17 show the plots obtained from FactSage™ simulation of a synthetic petcoke, the base composition of which was set to match the composition of LV sample, with different variations of the compositions and atmospheres forming the basis for the remaining plots. The plots depict the composition in moles (on y-axis) as a function of temperature (x-axis). To simulate the conditions that are encountered during viscosity measurement, two different phases of alumina -gamma and corundum, were included in the input to FactSage™. This was done solely based on their different melting points and stability at 1500˚C. Gamma alumina represents the powdered alumina in the slag and corundum is used for simulating the alumina from the crucible. Due to this setup, a comparison of the levels and rates of changes between these two components

would be indicative of the dissolution of powdered alumina and the crucible into the molten slag at different temperatures.

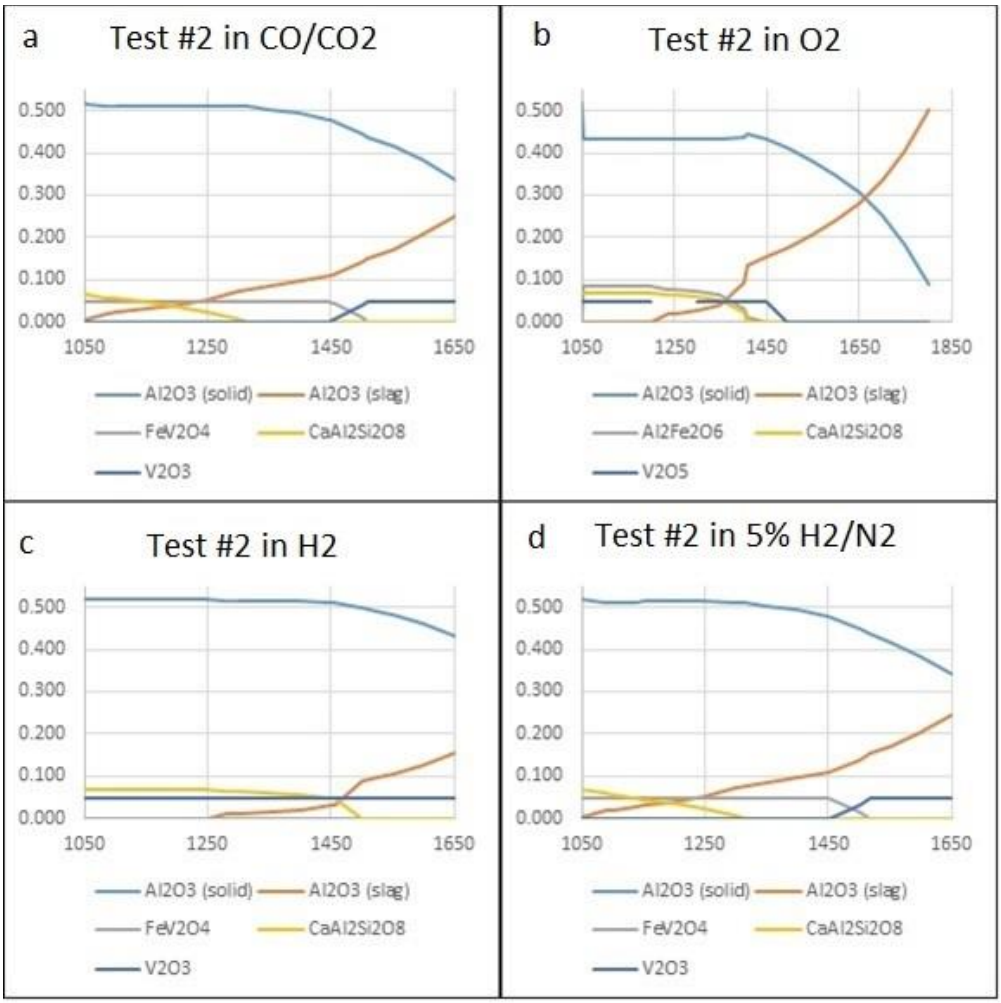

Figure 5-14 FactSage™ simulation of synthetic petcoke slag (LV composition).

The initial composition in Figure 5-14 is the same as that of LV and shows the effect of processing this slag under CO/CO_2 (69.5/30.5) (Figure 5-14 a), pure O_2 (Figure 5-14 b), pure H_2 (Figure 5-14 c), and H_2/N_2 (5/95 %) mix (Figure 5-14 d) atmospheres. The blue plots indicate the content of alumina in the crucible/ refractory as a function of temperature under the specified conditions, while the red plots show the content of alumina predicted to be present in the slag at equilibrium. As the crucible/ refractory dissolves, the blue plot is expected to drop, and the red plot is expected to rise.

Analysis of the four FactSage™ plots (Figure 5-14 a-d) shows that the dissolution of crucible is the maximum when the slag is processed under oxidizing conditions (pure O_2). At 1500˚C – the highest temperature that the slag was heated to during the viscosity measurement,

there exist about 0.17 moles of Al_2O_3 in the liquid slag at equilibrium. We would refer to these numbers as equilibrium henceforth. If a composition has lesser alumina in it than that predicted at equilibrium, it is called a sample deficit in alumina, else if it has higher alumina in the starting mix than predicted to be at equilibrium, it is called a sample with excess alumina. 0.04 moles of Al_2O_3 were added to the initial oxide mixture. As a result, we can see that there is a deficit of about 0.13 moles of Al_2O_3 in the liquid slag under oxidizing conditions (Figure 5-14b). Similarly, processing under CO/CO_2 atmosphere shows a deficit of 0.1 moles at 1500˚C, under pure H_2 atmosphere it comes down to 0.05 moles. This deficit could be the reason for the dissolution of the alumina.

The plots for V_2O_3 and FeV_2O_4 are symmetric and suggest that the drop in concentration of one is directly related to the rise in the concentration of the other. In Figure 5-14 a, c and d vanadium exists as FeV_2O_4 until about 1450˚C. Thereafter, it continues to be in the same form in pure H_2 atmosphere while dissociating into V_2O_3 in the remaining two atmospheres. These simulations show that the equilibrium content of alumina in the slag at 1650°C under oxidizing conditions is about 0.3 moles against 0.25 moles predicted under reducing conditions.

Figure 5-15 shows the simulation plot obtained for high alumina sample with composition like LV sample with 0.3 moles of alumina added to it against 0.04 moles earlier. All other components were retained at the same levels. The amount of additional alumina was decided based on the deficit observed in the previous simulation (Figures 5-14 a-d). It was seen that addition of alumina did not change the equilibrium content of alumina in the slag, as it remained the same as in previous case (Figure 5-14). It did however, lead to lesser dissolution of alumina from the crucible/ refractory. In the simulation carried out with LV composition, the loss of alumina was approximately 40% whereas it dropped to about 25% when excess alumina was added to the slag. FeV_2O_4 is predicted to exist until about 1450˚C before dissociating into V_2O_3.

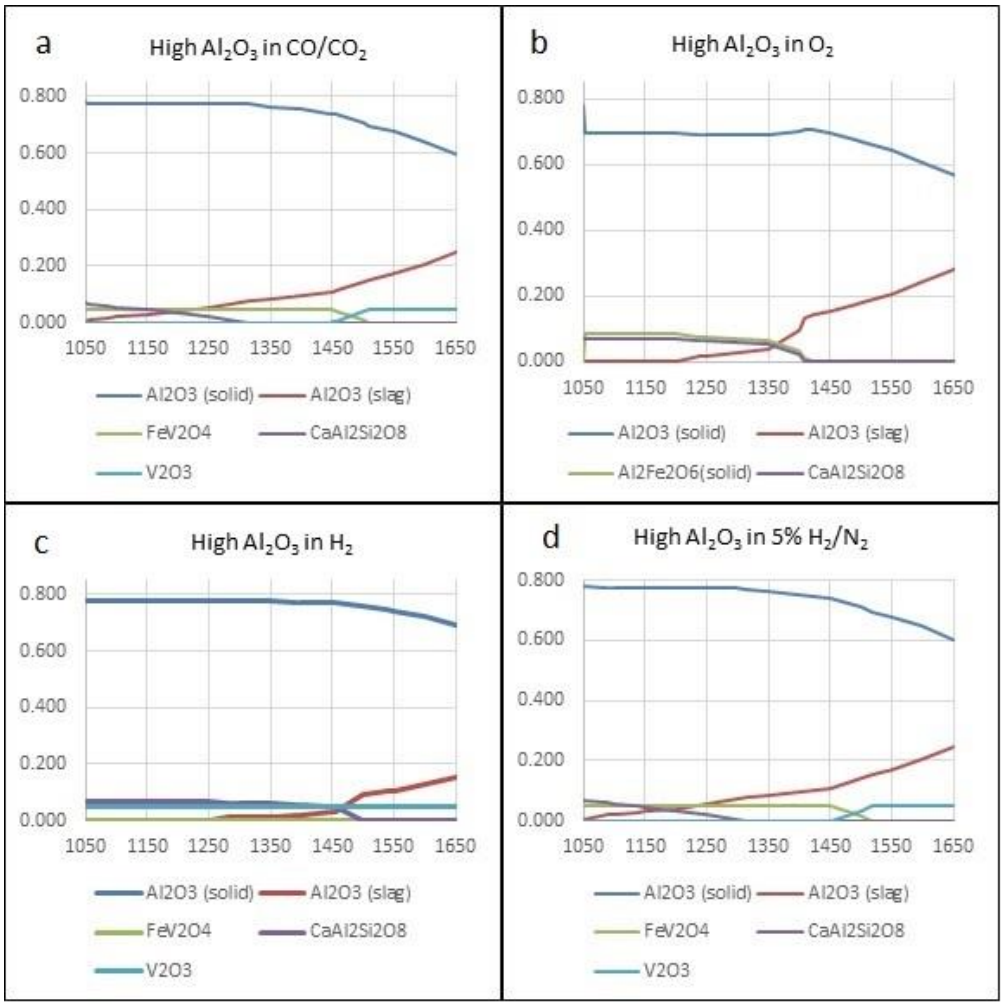

Figure 5-15 FactSage™ simulation of synthetic petcoke slag (high alumina).

Figure 5-16 shows FactSage™ results for a case with no alumina added to the initial oxide mix. This helps us understand how the lack of alumina in the starting mix affects the equilibrium quantity of alumina predicted by the software. Again, the equilibrium content of alumina is found to be the same as in previous cases. In all the cases simulated, alumina in the slag existed as anorthite at lower temperatures and dissociated at different temperatures depending on the atmosphere.

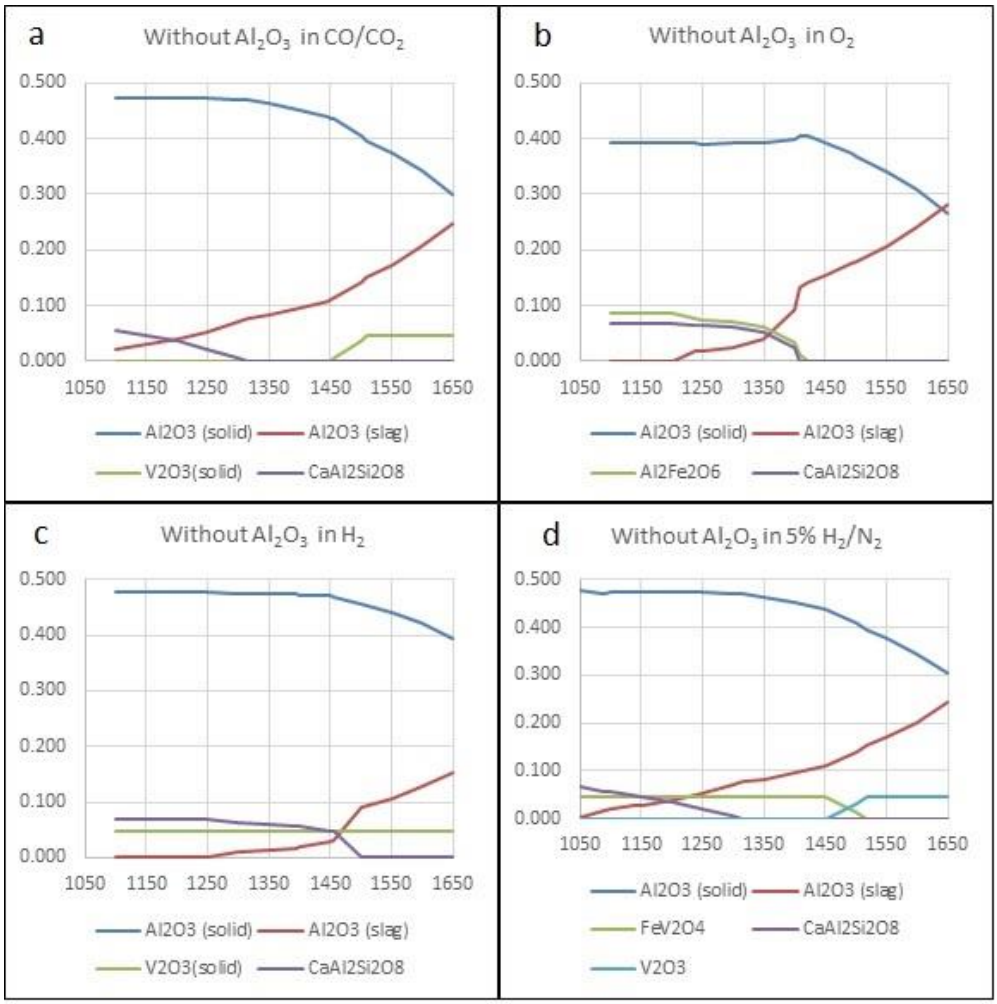

Figure 5-16 FactSage™ simulation of synthetic petcoke (no alumina).

Figure 5-17 shows the simulation of the synthetic petcoke slag with both alumina and vanadium absent. The dissolution of alumina into the slag is predicted to be similar to other cases and is not much affected in the absence of both these components. The dissolution of alumina from the crucible starts when the slag starts melting and continues until the system reaches equilibrium. This shows that when there is no alumina in the starting mixture, and the slag is melted in alumina crucibles, slag pick up alumina from the crucibles to reach thermodynamic equilibrium. The quantity of alumina picked up is dependent on the prevailing atmosphere and the slag temperature.

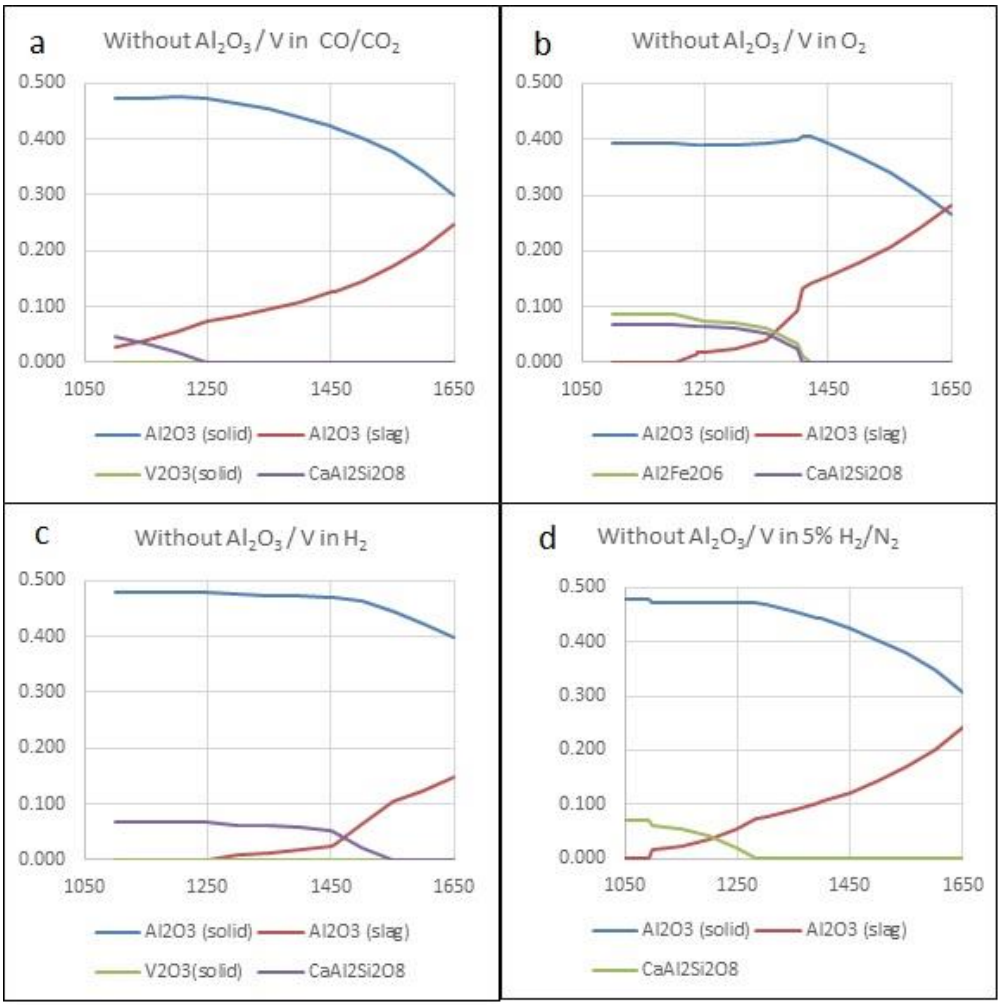

Figure 5-17 FactSage™ simulation of synthetic petcoke (no alumina/ vanadium).

From the sixteen simulations carried out (four compositions in four atmospheres each), it is clear that FactSage™ predicts lower dissolution of Al_2O_3 into the slag when processed under 100% H_2 atmosphere than when processed under an atmosphere of CO/ CO_2, which in turn shows less dissolution when compared to slags processed in O_2 atmosphere. Though H_2 provides the best atmosphere for preventing refractory dissolution, it also carries significant risk of explosion owing to the flammability of pure H_2.

The plots also show that under a given atmosphere and at a given temperature, the quantity of Al_2O_3 present in slag form at equilibrium is a constant. It is also clear that the prediction of formation of various compounds does not change when the CO/CO_2 atmosphere is replaced by 5% H_2 atmosphere. Dissolution is found to be of the same order in both the cases. Thus, 5%H_2/ N_2 gas mix may be used as a substitute for CO/CO_2 mix for carrying out experimental validation of FactSage™ results.

Another interesting observation from the FactSage™ simulations is that the dissociation of anorthite is closely related to the loss of alumina from the crucible. They both start simultaneously, with most of the alumina picked up by the slag coming from the dissociation of anorthite. Dissolution of alumina from crucible increased after complete dissociation of anorthite. This might indicate the slag's preference towards the different phases of alumina, especially alumina that is freely available (in powder form as part of slag). This preference strongly supports the assertion that slag starts dissolving alumina from the crucible when there is not enough of it in the initial mix.

Based on the simulations, it was hypothesized that the alumina content of the initial slag plays a role in dissolution of crucibles. To validate this hypothesis, a synthetic slag with the V test composition was heated to 1500˚C in the Carbolite furnace, held at that temperature for 6 hours and gradually cooled down. The crucible was then inspected visually to look for any signs of dissolution from the walls. The crucibles were then sectioned for carrying out SEM-EDS and XRD analyses (figure 5-18, 5-19 and 5-20).

Figure 5-18 shows the SEM micrograph of the wall of the crucible, close the interface with slag, while Figure 5-19 shows the EDS pattern for the surface. The image in Figure 5-18 shows that the wall of the crucible was not involved in any chemical reaction with the components of the slag, as seen by the absence of any interface/ multi-component regions. This was also corroborated by the EDS pattern generated at the same location (Figure 5-19). The percentage of aluminum by weight (26.3%) shows that there has been no degradation from this surface. Silicon content (12.8%) was slightly higher than in the starting mixture. This could be explained by the differences in densities of the components and the duration of time for which the sample was held at 1500˚C.

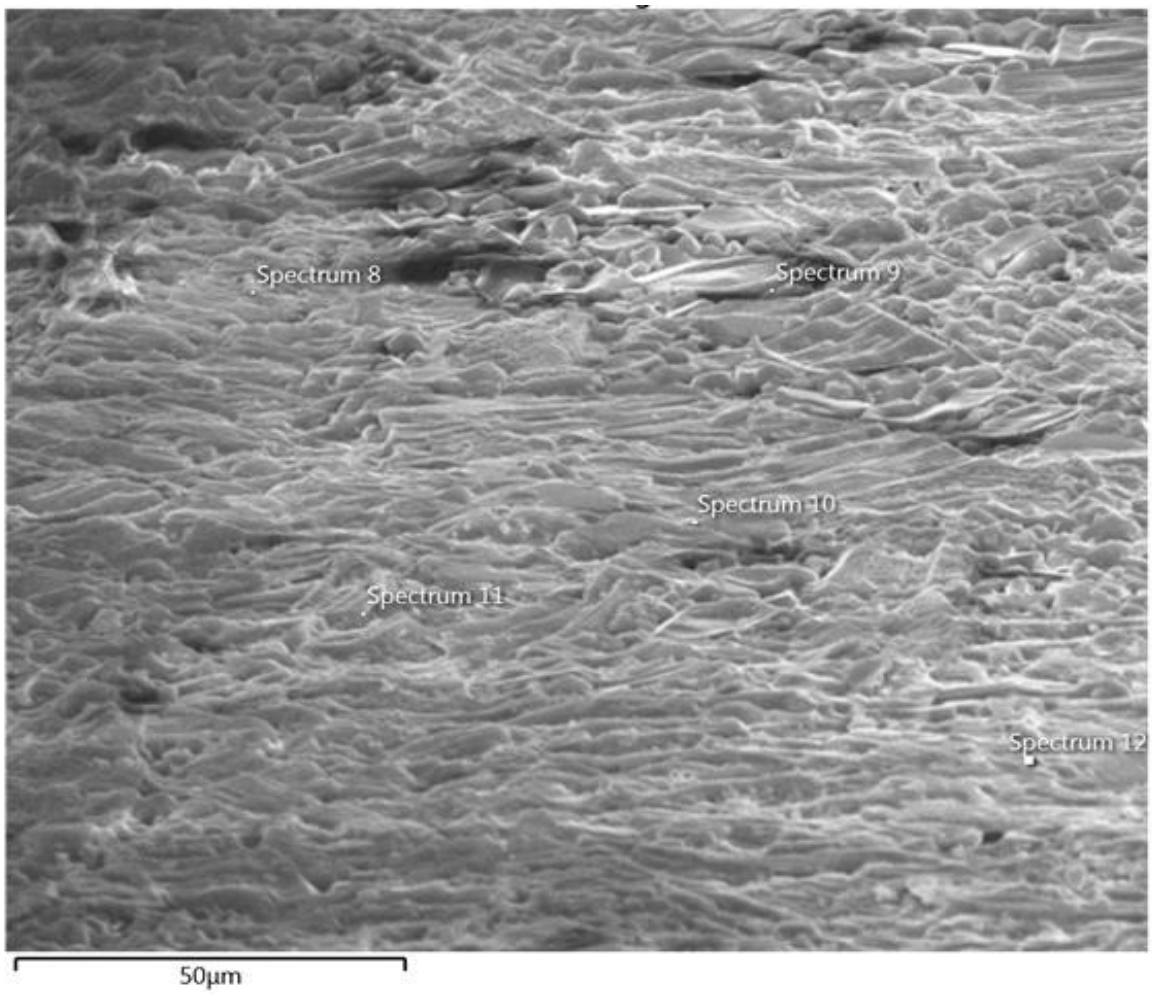

Figure 5-18 SEM micrograph of the crucible wall, close to the interface (V test)

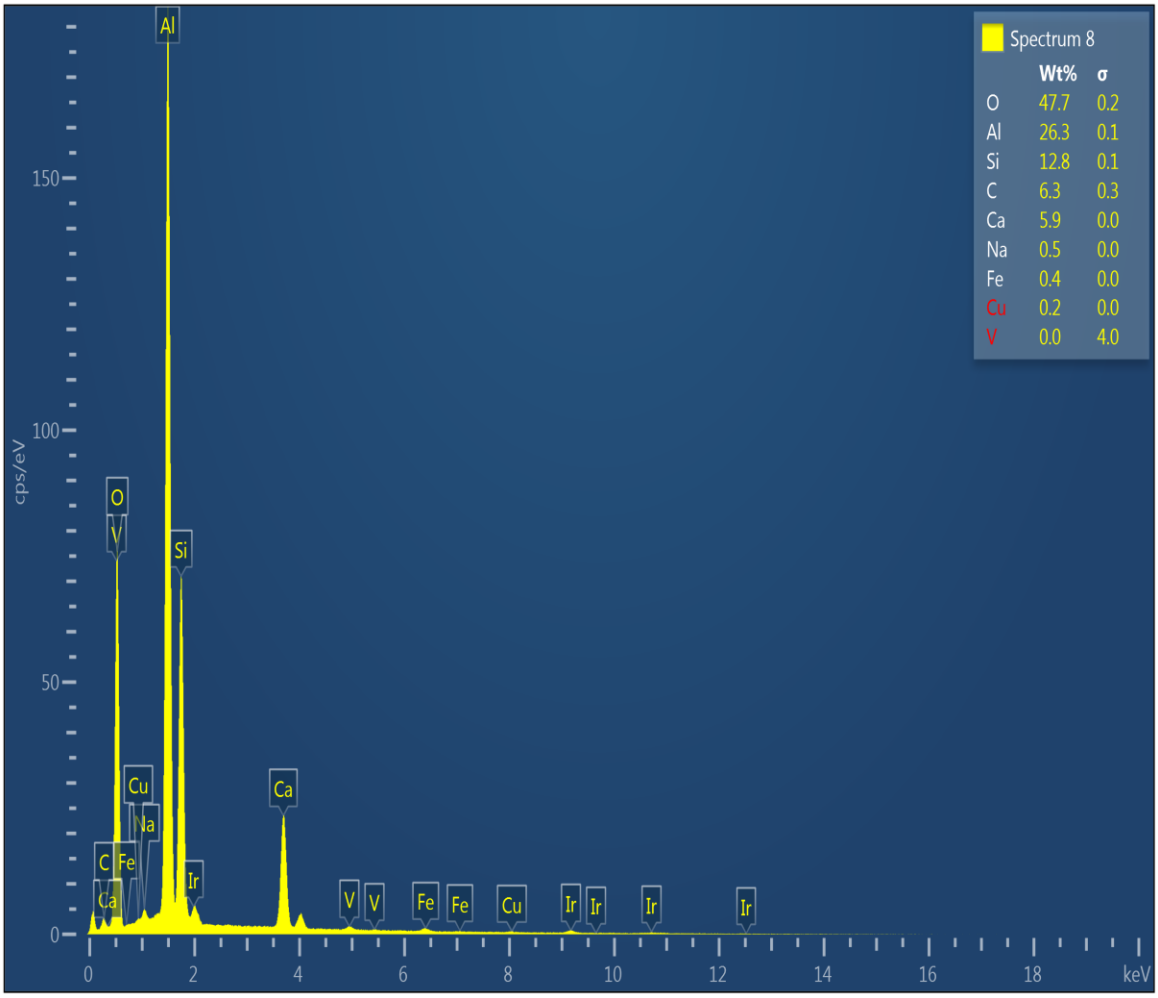

Figure 5-19 EDS pattern of the crucible close to interface (V test).

Figure 5-20 shows the plots obtained during XRD analysis of LV and V samples. A comparison shows that the plots are exactly similar but for the lack of a peak showing vanadium in LV sample (red plot), while there is evidence of presence of vanadium compound in a phase similar to magnesiocoulsonite (MgV_2O_4) in the validation test. This product could be FeV_2O_4 with Mg being replaced by Fe in the crystal structure. The lack of vanadium peaks in LV sample could also be explained by the fact that most of the slag from LV sample leaked out from the perforations in the crucible wall, thus depleting vanadium from the test sample. From the discussion above, we can conclude that 69.5% CO/ 30.5% CO_2 and 5% H_2 atmospheres have a similar effect on the oxide mixture and can be used interchangeably.

The presence of vanadium in the validation test agrees with the prediction made by FactSage™ that V exists as FeV_2O_4 through about 1450˚C under reducing conditions. FactSage™ also correctly predicts the presence of most of gamma alumina as anorthite. Furthermore, no

evidence of V_2O_3 was found from the XRD plots, indicating that formation of V_2O_3 is not favored thermodynamically under the conditions of the test, again in agreement with the predictions made by FactSage™. Formation of V_2O_3 could possibly be dependent on the starting concentration of Fe_2O_3 added to the oxide mix, as any oxide not dissolving into slag or present as metallic Fe would likely form FeV_2O_4. However, above 1500°C, all the Fe in the system is present in body centered cubic structure in its metallic form in the slag. This coincides with the transformation of FeV_2O_4 to V_2O_3. The probable reaction involved in this process would be

$$2\ FeV_2O_4 \longrightarrow 2\ Fe\ (bcc) + 2\ V_2O_3 + O_2$$

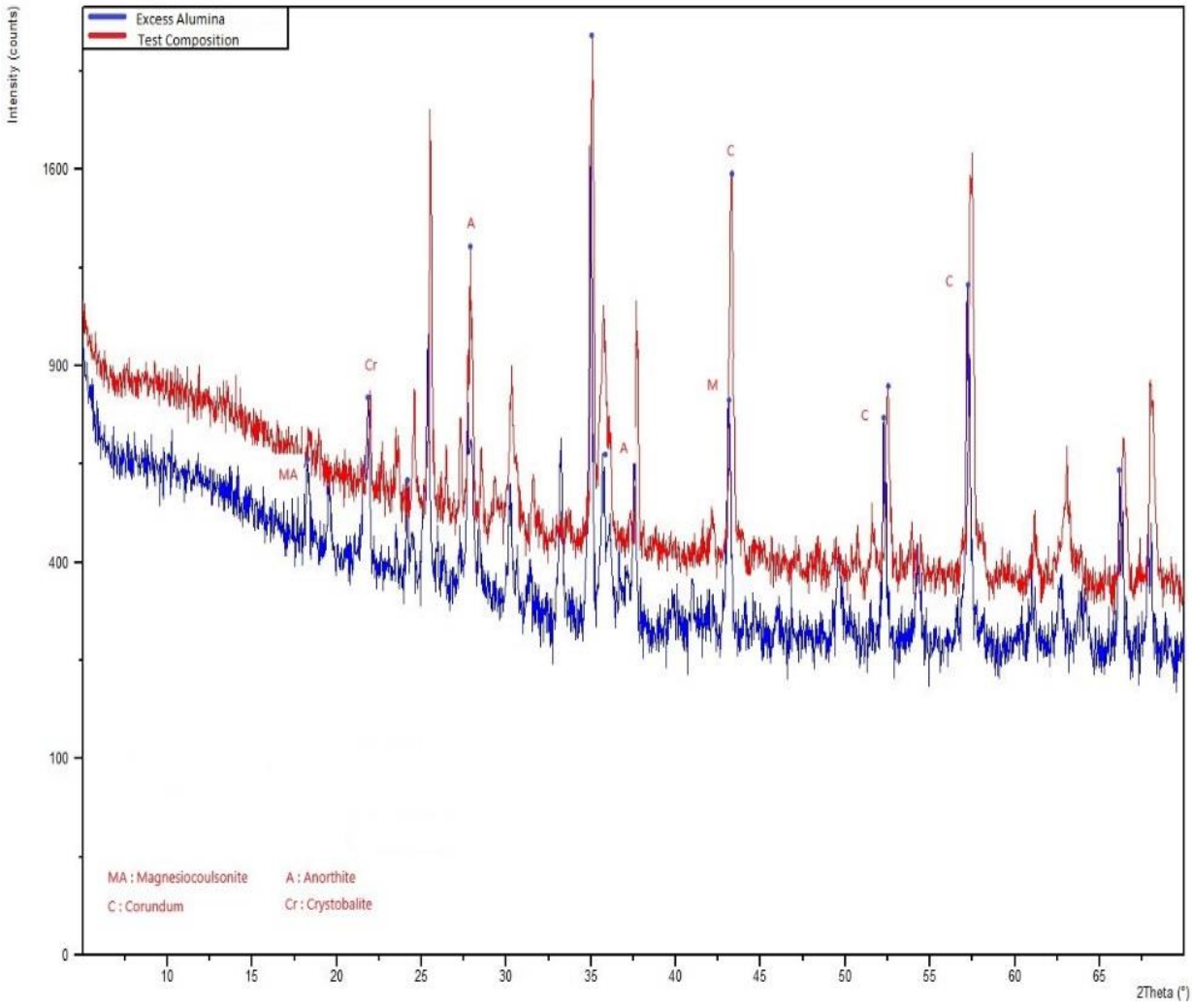

Figure 5-20 XRD plots for LV and V tests.

Further simulations were carried out for different concentrations of H_2 in H_2/N_2 mixture (10%, 20%, 25%, 50%, and 75%) with the same slag composition (V sample) to observe its influence on the prediction. The plots obtained from the simulation are shown below (Figure 5-21 through 5-25).

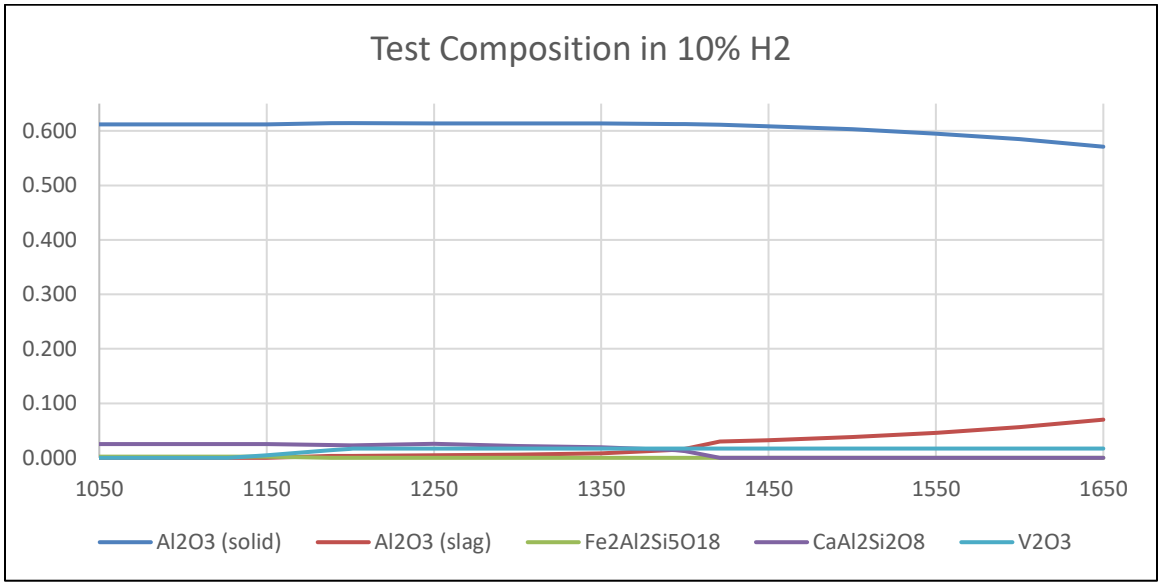

Figure 5-21 V Test Composition in 10% H_2

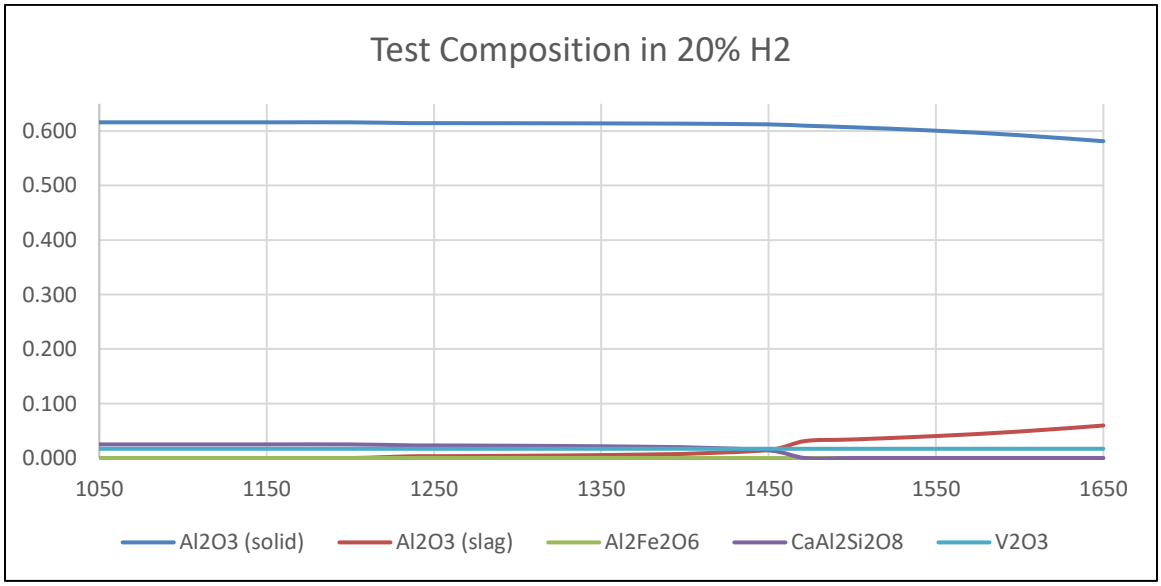

Figure 5-22 V Test Composition in 20% H_2

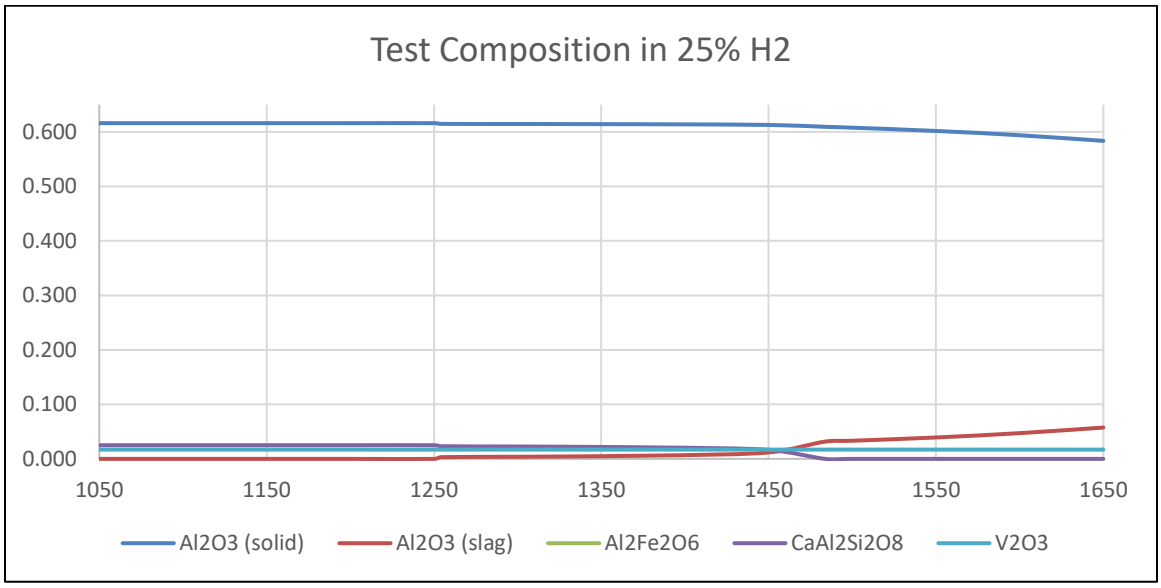

Figure 5-23 V Test Composition in 25% H_2

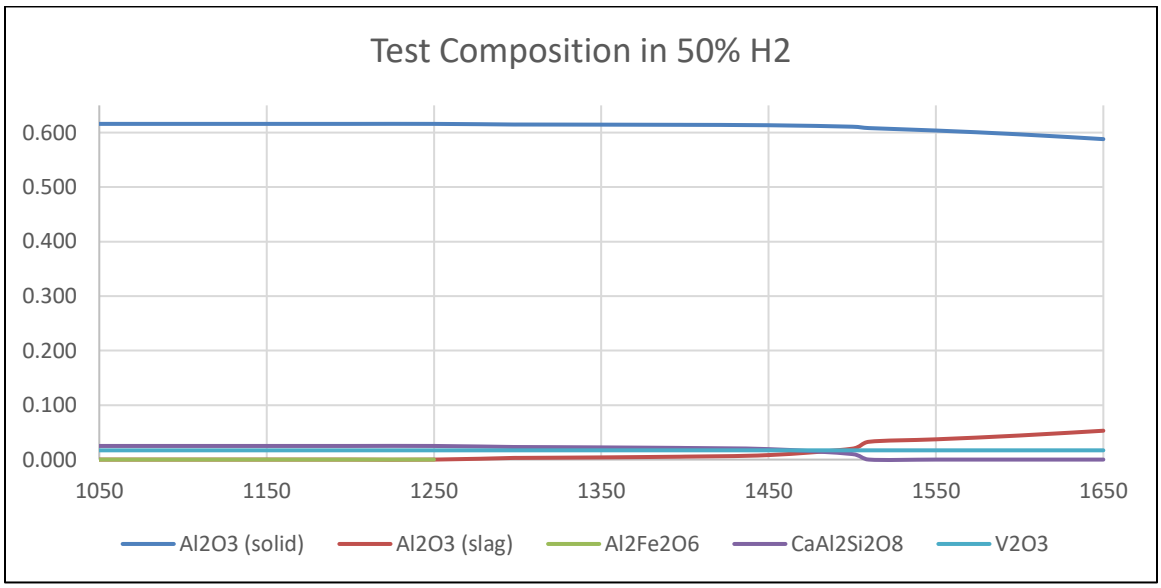

Figure 5-24 V Test Composition in 50% H_2

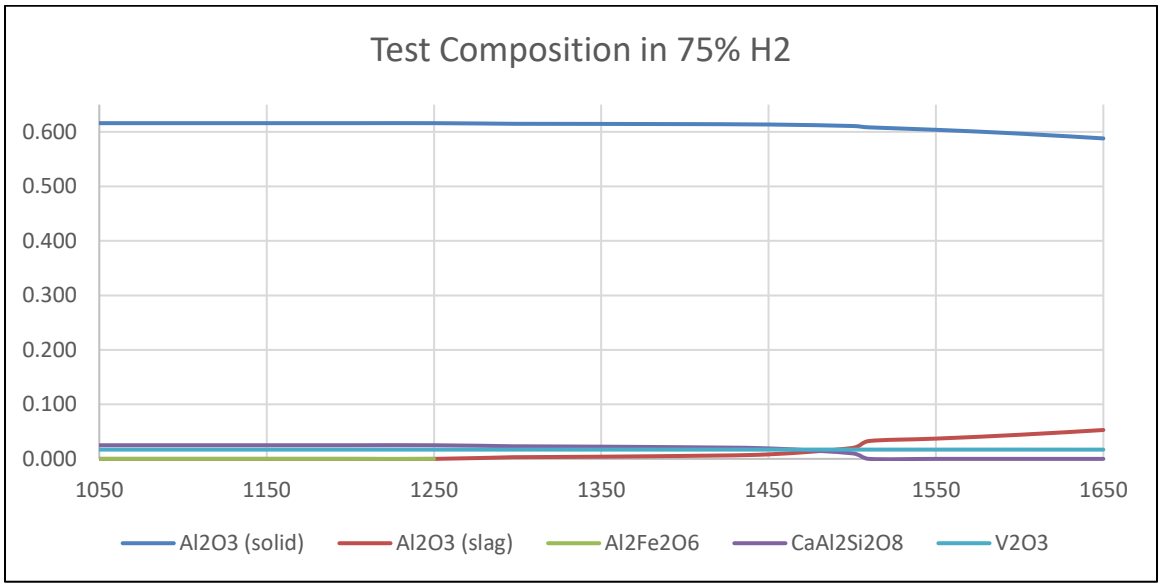

Figure 5-25 V Test Composition in 75% H_2

The five figures above (Figure 5-21 through 5-25) clearly show that the change in concentration of H_2 has minimal bearing on the dissolution of alumina into the slag. A change from 10% H_2 (figure 5-21) to 75% H_2 (Figure 5-25) does not change the dissolution of the crucible appreciably.

Analysis of alumina dissolution under 5% H_2 and 100% H_2 atmospheres for various compositions (Figures 5-14, 5-15, 5-16, and 5-17) shows that the maximum dissolutions of alumina (at 1650°C) were about 9.25% and 4.41% respectively. However, the safety risk posed by the presence of higher concentrations of highly inflammable hydrogen make 5% hydrogen a better choice for providing reducing atmospheres.

Chapter 6
CONCLUSIONS

The reasons for dissolution of alumina from the crucible into the molten slags while measuring their viscosities were investigated. The slag composition was modeled using FactSage™ under different atmospheres and the equilibrium amount of alumina in the slag in the range 1050˚C-1650˚C was obtained. XRD analysis of the slag sample revealed that vanadium exists as FeV_2O_4 and not as V_2O_3 at temperatures lower than 1450˚C.

The dissolution of alumina from the wall into the slag was found to be minimum under reducing conditions and maximum under oxidizing conditions. Oxidizing atmosphere promoted dissolution of alumina into the slag by promoting faster dissociation of anorthite, followed by dissolution of alumina from the crucible. H_2 and CO/ CO_2 provided similar types of reducing atmospheres during the experiment.

Simulations carried out with varying contents of alumina showed that the initial alumina content in the slag mixture has no effect on the equilibrium content in the molten slag. The deficit of alumina in the slag is compensated by the dissolution of alumina from the crucible. SEM data showed that slags with excess alumina did not cause any identifiable dissolution.

It is thus suggested that slags with low alumina content in the ash would benefit by addition of excess of alumina during operation to minimize the dissolution from the crucible/ reactor walls. The quantity of alumina to be added can be determined by simulation in FactSage™.

Excess alumina in a slag can cause an increase in its viscosity. This could lead to greater degradation of the refractory due to increased contact time with the hot slag. Thus, there could be an optimum quantity of alumina to be added to the slag to mitigate refractory dissolution as well as minimizing the rise in viscosity. Further research is required to understand the mechanism of slag-refractory interactions better. Besides vanadium, nickel is another major constituent of petcoke ash slags. There is limited literature on the role of nickel in the phenomenon of refractory dissolution into slag. Further research needs to be directed at understanding the role played by nickel.

Further study is required to understand the effect of ferric oxide content in the slag on the interaction between vanadium and alumina. If it does affect the reactivity of vanadium, it could pave way for using unblended petcoke in gasifiers.

Understanding the mechanism of refractory dissolution into slag would contribute to development of materials better suited for high-temperature applications, especially gasifier linings for improving the reliability of gasifiers which has been a challenge for this technology.

REFERENCES

[1] B. N. Murthy, A. N. Sawarkar, N. A. Deshmukh, T. Mathew, and J. B. Joshi, "Petroleum coke gasification: A review," *Canadian Journal of Chemical Engineering*, vol. 92, no. 3, pp. 441–468, 2014.

[2] J. P. Bennett and K. S. Kwong, "Failure mechanisms in high chrome oxide gasifier refractories," *Metallurgical and Materials Transactions A Physical Metallurgy and Material. Science*, vol. 42, no. 4, pp. 888–904, 2011.

[3] F. Frandsen, K. Dam-Johansen, and P. Rasmussen, "Trace elements from combustion and gasification of coal-An equilibrium approach," *Progress in Energy and Combustion Science*, vol. 20, no. 2, pp. 115–138, 1994.

[4] R. W. Bryers, "Utilization of petroleum coke and petroleum coke/coal blends as a means of steam raising," *Fuel Processing Technology*, vol. 44, no. 1–3, pp. 121–141, 1995.

[5] S. Vargas, F. J. Frandsen, and K. Dam-Johansen, "Rheological properties of high-temperature melts of coal ashes and other silicates," *Progress in Energy and Combustion Science*, vol. 27, no. 3, pp. 237–429, 2001.

[6] B. C. Folkedahl and H. H. Schobert, "Effects of atmosphere on viscosity of selected bituminous and low-rank coal ash slags," *Energy and Fuels*, vol. 19, no. 1, pp. 208–215, 2005.

[7] J. Zhu, T. K. Kaneko, H. Mu, J. P. Bennett, and S. Sridhar, "Effects of measurement materials and oxygen partial pressure on the viscosity of synthetic eastern and western United States coal slags," *Energy and Fuels*, vol. 26, no. 7, pp. 4465–4474, 2012.

[8] J. P. Hurley, T. M. Wame, and J. W. Nowok, "Slag viscosity," pp. 691–694.

[9] Y. Kim and M. S. Oh, "Effect of cooling rate and alumina dissolution on the determination of temperature of critical viscosity of molten slag," *Fuel Processing Technology*, vol. 91, no. 8, pp. 853–858, 2010.

[10] J. Nakano, M. Duchesne, J. Bennett, K. S. Kwong, A. Nakano, and R. Hughes, "Thermodynamic effects of calcium and iron oxides on crystal phase formation in synthetic gasifier slags containing from 0 to 27 wt.% V2O3," *Fuel*, vol. 161, pp. 364–375, 2015.

[11] J. Zhou, Z. Shen, Q. Liang, J. Xu, and H. Liu, "A new prediction method for the viscosity of the molten coal slag. Part 1: The effect of particle morphology on the suspension viscosity," *Fuel*, vol. 220, no. November 2017, pp. 296–302, 2018.

[12] J. Zhou, Z. Shen, Q. Liang, J. Xu, and H. Liu, “A new prediction method for the viscosity of the molten coal slag. Part 2: The viscosity model of crystalline slag,” *Fuel*, vol. 220, no. November 2017, pp. 233–239, 2018.

[13] G. J. Browning, G. W. Bryant, H. J. Hurst, J. A. Lucas, and T. F. Wall, “An empirical method for the prediction of coal ash slag viscosity,” *Energy and Fuels*, vol. 17, no. 3, pp. 731–737, 2003.

[14] M. A. Duchesne *et al.*, “Flow behaviour of slags from coal and petroleum coke blends,” *Fuel*, vol. 97, pp. 321–328, 2012.

[15] Z. Wang *et al.*, “Viscosity of coal ash slag containing vanadium and nickel,” *Fuel Processing. Technology*, vol. 136, pp. 25–33, 2015.

[16] P. Y. Hsieh, K. S. Kwong, and J. Bennett, “Correlation between the critical viscosity and ash fusion temperatures of coal gasifier ashes,” *Fuel Processing. Technology*, vol. 142, pp. 13–26, 2016.

[17] X. Liu, G. Yu, J. Xu, Q. Liang, and H. Liu, “Viscosity fluctuation behaviors of coal ash slags with high content of calcium and low content of silicon,” *Fuel Processing. Technology*, vol. 158, pp. 115–122, 2017.

[18] S. Srinivasachar, C.L Senior, J.J.Helble and J.W.Moore, “A Fundamental Approach To The Prediction Of Coal Ash Deposit Formation In Ccombustion Systems,” vol. 102, no. July 1985, pp. 452–458, 1986.

[19] H. J. Hurst, J. H. Patterson, and A. Quintanar, “Viscosity measurements and empirical predictions for some model gasifier slags - II,” *Fuel*, vol. 79, no. 14, pp. 1797–1799, 2000.

[20] H. J. Hurst, F. Novak, and J. H. Patterson, “Viscosity measurements and empirical predictions for fluxed Australian bitumnous coal ashes,” *Fuel*, vol. 78, pp. 1831–1840, 1999.

[21] A. Kondratiev, E. Jak, and P. C. Hayes, “Predicting slag viscosities in metallurgical systems,” *Jom*, vol. 54, no. 11, pp. 41–45, 2002.

[22] M. Kim, I. Ye, and C. Ryu, “Effect of slag viscosity model on transient simulations of wall slag flow in an entrained coal gasifier,” *Korean Journal of Chemical Engineering*, vol. 35, no. 5, pp. 1065–1072, 2018.

[23] M. S. Oh, D. D. Brooker, E. F. de Paz, J. J. Brady, and T. R. Decker, “Effect of crystalline phase formation on coal slag viscosity,” *Fuel Processing Technology*, vol. 44, no. 1–3, pp. 191–199, 1995.

[24] S. Mueller, E. W. Llewellin, and H. M. Mader, “The effect of particle shape on suspension viscosity and implications for magmatic flows,” *Geophysical Research Letters*, vol. 38, no.

13, pp. 1–5, 2011.

[25] F. Vetere, H. Behrens, F. Holtz, G. Vilardo, and G. Ventura, “Viscosity of crystal-bearing melts and its implication for magma ascent,” *Journal of Mineralogical and Petrological Sciences*, vol. 105, no. 3, pp. 151–163, 2010.

[26] A. Costa, “Viscosity of high crystal content melts: Dependence on solid fraction,” *Geophysical Research Letters*, vol. 32, no. 22, pp. 1–5, 2005.

[27] J. C. van Dyk, F. B. Waanders, S. A. Benson, M. L. Laumb, and K. Hack, “Viscosity predictions of the slag composition of gasified coal, utilizing FactSage equilibrium modelling,” *Fuel*, vol. 88, no. 1, pp. 67–74, 2009.

[28] P. Wang and M. Massoudi, “Slag behavior in gasifiers. Part I: Influence of coal properties and gasification conditions,” *Energies*, vol. 6, no. 2, pp. 784–806, 2013.

[29] M. Massoudi and P. Wang, *Slag behavior in gasifiers. Part II: Constitutive modeling of slag*, vol. 6, no. 2. 2013.

[30] A. Y. Ilyushechkin, M. A. Duchesne, S. S. Hla, A. MacChi, and E. J. Anthony, “Interactions of vanadium-rich slags with crucible materials during viscosity measurements,” *Journal of Mateials Science*, vol. 48, no. 3, pp. 1053–1066, 2013.

[31] D. French, H. J. Hurst, and P. Marvig, “Comments on the use of molybdenum components for slag viscosity measurements,” *Fuel Processing Technology*, vol. 72, no. 3, pp. 215–225, 2001.

[32] R. E. Conn, “Laboratory techniques for evaluating ash agglomeration potential in petroleum coke fired circulating fluidized bed combustors,” *Fuel Processing Technology*, vol. 44, no. 1–3, pp. 95–103, 1995.

[33] S. V. Vassilev, C. Braekman-Danheux, R. Moliner, I. Suelves, M. J. Lázaro, and T. Thiemann, “Low cost catalytic sorbents for NOxreduction - 1. Preparation and characterization of coal char impregnated with model vanadium components and petroleum coke ash,” *Fuel*, vol. 81, no. 10, pp. 1281–1296, 2002.

[34] C. H. Lindsley and E. K. Fischer, “End-effect in rotational viscometers,” *Journal of Applied Physics*, vol. 18, no. 11, pp. 988–996, 1947.

APPENDIX A

Modified Urbain Equation

The equation used for determination of viscosity is:

$$\eta = a\ T\ e^{(b.\ 1000)/T},$$

Where a and b are adjustable parameters dependent on the composition of the melt and T is the temperature at which viscosity is being estimated.

Further, the relationship between a and b is determined using the following equation:

$$-\ln a = 0.2693\ b + 13.9751$$

Computation of b is done from the composition of the melt as below:

$$b = b_0 + b_1\ (SiO_2) + b_2\ (SiO_2)^2 + b_3\ (SiO_2)^3,$$

Where the coefficients are computed from the values of α as below:

$$b_0 = 13.8 + 39.9355\ \alpha - 44.049\ \alpha^2$$

$$b_1 = 30.481 - 117.1505\ \alpha + 129.9978\ \alpha^2$$

$$b_2 = -40.9429 + 234.0486\ \alpha - 300.04\ \alpha^2$$

$$b_3 = 60.7619 - 153.9276\ \alpha + 211.1616\ \alpha^2$$

The value of α for use in the equation above is found out by using the following relation

$$\alpha = x_m/(x_m + x_a),$$

Where,

$x_g = SiO_2 + P_2O_5$;

$x_m = FeO + CaO + MgO + Na_2O + K_2O + MnO + NiO + 2(TiO_2 + ZrO_2) + 3\ CaF_2$;

$x_a = Al_2O_3 + Fe_2O_3 + B_2O_3$;

The terms in the above equations are

x_g : mole fraction (total) of glass forming oxides,

x_m : mole fraction (total) of glass modifier oxides, and

x_a : mole fraction (total) of amphoteric oxides

In the equations above, the chemical formulae of the oxides are used to represent the mole fraction of the respective oxides in the slag mixture.

APPENDIX B

Glossary of Terms

F	shear stress applied to the liquid
A	area over which the stress is being applied
v	velocity of the top surface of the liquid
t	fluid film thickness
Pa.s	Pascal second (unit of coefficient of dynamic viscosity
AFT	ash fusion temperature
T_{CV}	temperature of critical viscosity
η	viscosity, as measured using the modified Urbain equation
a, b	parameters, dependent on the slag composition
T	temperature of interest, at which viscosity needs to be predicted
$\mu_{mixture}$	viscosity of a fluid-suspended solid system (Annen equation)
μ_{liquid}	viscosity of a pure liquid (Annen equation)
c	theoretical solid volume fraction (Annen equation)
Φ	particle volume fraction
ϕ_m	maximum possible particle volume fraction

SEM-EDS	scanning electron microscopy-energy dispersive spectroscopy
XRD	x-ray diffraction
calibration sample	slag sample with composition based on the published literature
HV sample	slag sample with high content of vanadium
LV sample	slag sample with low content of vanadium
validation sample	LV sample with additional alumina